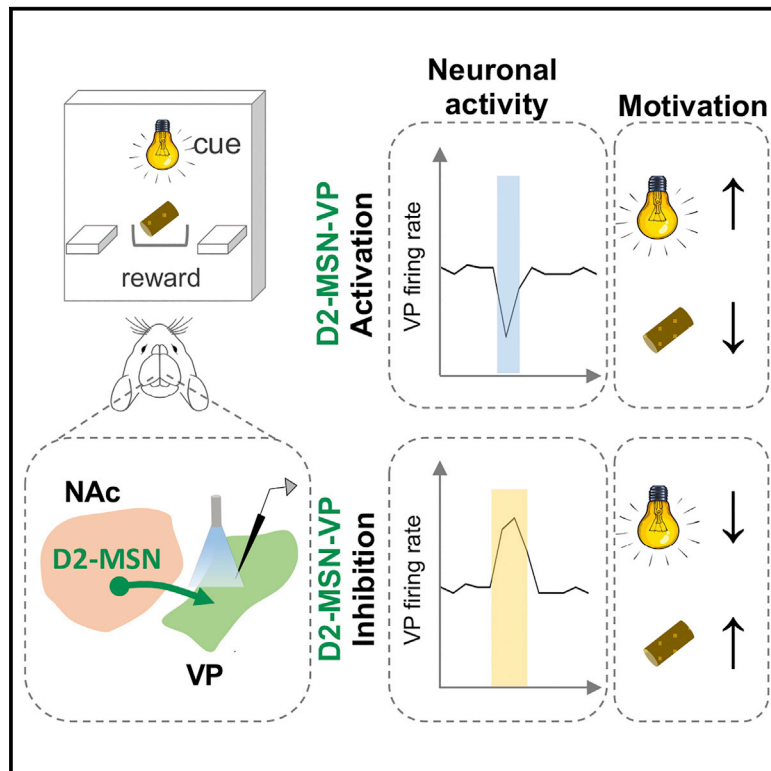


Distinct role of nucleus accumbens D2-MSN projections to ventral pallidum in different phases of motivated behavior

Graphical abstract



Authors

Carina Soares-Cunha,
Ana Verónica Domingues,
Raquel Correia, ..., Luísa Pinto,
Nuno Sousa, Ana João Rodrigues

Correspondence

carinacunha@med.uminho.pt (C.S.-C.),
ajrodrigues@med.uminho.pt (A.J.R.)

In brief

Soares-Cunha et al. show that optogenetic modulation of nucleus accumbens D2-MSN to ventral pallidum projections during different stages of motivated behavior has contrasting effects in motivation: cue-paired optical activation of D2-MSN-VP inputs increases motivation to work for food, whereas reward-paired activation reduces motivation.

Highlights

- Increased D2-MSN-VP activity during reward-predicting cue enhances motivation
- Suppression of D2-MSN-VP activity during reward consumption increases motivation



Report

Distinct role of nucleus accumbens D2-MSN projections to ventral pallidum in different phases of motivated behavior

Carina Soares-Cunha,^{1,2,*} Ana Verónica Domingues,^{1,2} Raquel Correia,^{1,2} Bárbara Coimbra,^{1,2} Natacha Vieitas-Gaspar,^{1,2} Nivaldo A.P. de Vasconcelos,^{1,2,3,4} Luísa Pinto,^{1,2} Nuno Sousa,^{1,2,5} and Ana João Rodrigues^{1,2,6,*}

¹Life and Health Sciences Research Institute (ICVS), School of Medicine, University of Minho, Braga, Portugal

²ICVS/3B's-PT Government Associate Laboratory, Braga, Portugal

³Physics Department, Federal University of Pernambuco (UFPE), Recife, Pernambuco 50670-901, Brazil

⁴Department of Biomedical Engineering, Federal University of Pernambuco (UFPE), Recife, Pernambuco 50670-901, Brazil

⁵Clinical Academic Center-Braga (2CA), Braga, Portugal

⁶Lead contact

*Correspondence: carinacunha@med.uminho.pt (C.S.-C.), ajrodrigues@med.uminho.pt (A.J.R.)

<https://doi.org/10.1016/j.celrep.2022.110380>

SUMMARY

The nucleus accumbens (NAc) is a key region in motivated behaviors. NAc medium spiny neurons (MSNs) are divided into those expressing dopamine receptor D1 or D2. Classically, D1- and D2-MSNs have been described as having opposing roles in reinforcement, but recent evidence suggests a more complex role for D2-MSNs. Here, we show that optogenetic modulation of D2-MSN to ventral pallidum (VP) projections during different stages of motivated behavior has contrasting effects in motivation. Activation of D2-MSN-VP projections during a reward-predicting cue results in increased motivational drive, whereas activation at reward delivery decreases motivation; optical inhibition triggers the opposite behavioral effect. In addition, in a free-choice instrumental task, animals prefer the lever that originates one pellet in opposition to pellet plus D2-MSN-VP optogenetic activation and vice versa for optogenetic inhibition. In summary, D2-MSN-VP projections play different, and even opposing, roles in distinct phases of motivated behavior.

INTRODUCTION

The nucleus accumbens (NAc) is key in regulating reward-seeking and motivated behaviors (Berridge, 2012; Soares-Cunha et al., 2016a). *In vivo* electrophysiological studies show that NAc neurons encode both the predictive value of environmental stimuli and the specific motor behaviors required to respond to them (Carelli, 2002; Nicola et al., 2004). Interestingly, with learning, NAc neurons, particularly those located in the core, develop responses to cues predicting rewards (Ambroggi et al., 2011).

The NAc receives dopamine (but not only) signals from the ventral tegmental area (VTA), which acts predominantly via D1 or D2 dopamine receptors that are expressed by largely non-overlapping populations of medium spiny neurons (MSNs) (Gerfen and Surmeier, 2011). These two MSN sub-populations project to different outputs: D1-MSNs project to the VTA, while both D1- and D2-MSNs project to the ventral pallidum (VP) (Kupchik et al., 2015; Lu et al., 1997). Initial studies suggested that different NAc MSN subtypes play distinct and opposing roles in motivated behaviors: optical activation of D1-MSNs is rewarding, while activation of D2-MSNs is aversive (Kravitz et al., 2012; Lobo et al., 2010). However, other studies challenged this opposing view and showed that NAc D2-MSN optical stimulation promotes self-stimulation (Cole et al., 2018). In addition, we showed that brief optical

activation of D2-MSNs paired with a reward-predicting cue enhances motivation to obtain food rewards (Soares-Cunha et al., 2016b, 2018). Part of this behavioral effect was triggered by a transient decrease in the activity of VP GABAergic neurons that resulted in the disinhibition of VTA dopaminergic activity (Soares-Cunha et al., 2018, 2020), which is known to increase motivational levels (Ferguson et al., 2020; Ilango et al., 2014; Mohebi et al., 2019). However, others showed that chemogenetic inhibition of D2-MSNs during a progressive ratio task enhances motivation, without affecting sensitivity for reward devaluation (Carvalho Poyraz et al., 2016), and causes animals to initiate more frequently behavior without goal-directed efficiency (Gallo et al., 2018), an effect caused by disinhibition of VP GABAergic activity (Gallo et al., 2018). These studies and others support the importance of NAc-VP inputs and that VP is a critical interface between reward processing and motor output (Chang et al., 2018; Ottenheimer et al., 2018).

Previous data presented conflicting results regarding D2-MSNs' role in motivation (Carvalho Poyraz et al., 2016; Cole et al., 2018; Gallo et al., 2018; Soares-Cunha et al., 2016b, 2018), suggesting that these neurons play distinct roles in different stages of motivated behavior. Thus, in order to better understand the contribution of D2-MSN-VP projections in reward-related behaviors, we performed optical manipulation of these inputs during specific segments of behavior. We show



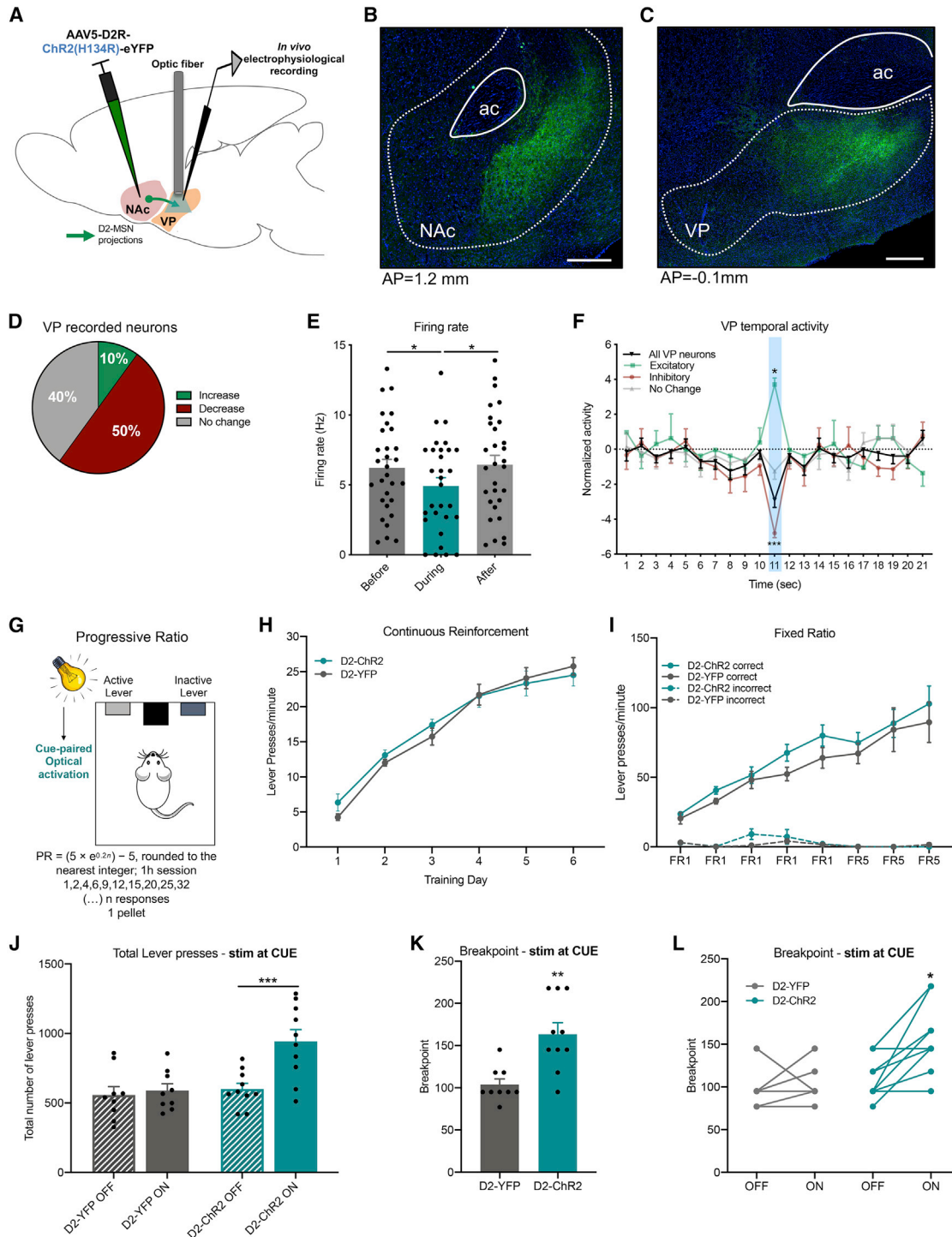


Figure 1. Optogenetic activation of D2-MSN-VP terminals during cue exposure increases motivation

(A) Strategy used for NAc D2-MSN-VP projection optogenetic stimulation and electrophysiological recordings in the VP.

(B and C) Representative immunofluorescence for YFP expression (B) in the NAc and (C) in terminals in the VP; scale bars represent 400 μ m; AP, anteroposterior.

(D) Pie chart of VP neurons responding to D2-MSN optical stimulation (473 nm, 1 s at 20 Hz, 25-ms light pulses, and 50% duty cycle).

(E) VP firing rate ($n = 30$ neurons/4 rats) in baseline, during optical stimulation, and afterward.

(F) Peristimulus time histogram (PSTH) of temporal variation of the normalized activity of VP neurons that increase (green; $n = 3$ neurons), decrease (red; $n = 15$ neurons), and do not change activity (gray; $n = 12$ neurons) during the stimulation period (blue).

(G) Schematic representation of the PR session with optogenetic activation of D2-MSN-VP (20 pulses of 25 ms at 20 Hz) at cue light presentation.

(legend continued on next page)

that D2-MSN-VP projections bidirectionally modulate motivated behavior, depending on the timing of stimulation: activation of D2-MS-VP inputs during cue exposure increases motivation, while activation at reward delivery decreases motivation in distinct behavioral paradigms.

RESULTS

Optogenetic activation of D2-MSN terminals modulates ventral pallidum activity

We unilaterally injected an AAV5 containing channelrhodopsin (ChR2) in fusion with enhanced yellow fluorescent protein (EYFP) under the control of the dopamine receptor D2 minimal promoter in the NAc of wild-type rats (D2-ChR2 group; Figure 1A), which allows specific manipulation of D2⁺ neurons. Control group was injected with an AAV containing EYFP (D2-YFP; Figures S1A and S1B). Expression of YFP was observed in cell bodies in the NAc (Figure 1B) and in D2-MSN terminals in the VP (Figure 1C). Viral specificity was also confirmed (Figure S1C), and results were in line with those previously reported for this viral construct (Soares-Cunha et al., 2018; Zalocusky et al., 2016).

We next used single-cell *in vivo* electrophysiology in anesthetized rats to evaluate optically evoked response of VP neurons to D2-MSN terminal activation (473 nm, 1 s at 20 Hz, 20 pulses of 25 ms, 50% duty cycle; 10 mW at the tip of the implanted fiber; Figure 1D). Half of VP recorded neurons decreased firing rate (considering the criteria of <20% below average baseline activity), 10% increased firing rate (at least >20% above average baseline activity), and 40% presented no change in comparison with baseline (Figure 1D). As a consequence, the net firing rate of VP significantly decreased during stimulation in comparison with baseline activity (Figure 1E; $p = 0.0339$). We also grouped neurons according to their type of response to the optical stimulation: increased activity; decreased activity; and no change in activity. As depicted in Figure 1F, excitatory and inhibitory responses were time locked to the stimulation period. After stimulation, VP firing rate returned to baseline levels ($p = 0.608$).

Cue-paired optogenetic activation of D2-MSN-VP projections increases motivation

To better understand the role of D2-MSN-VP terminals in motivated behaviors, we tested D2-ChR2 animals in a progressive-ratio (PR) task that has one lever associated with reward delivery (correct lever) and another lever that yields no reward (incorrect lever; Figure 1G). Each trial begins with turning ON of a cue light located above the correct lever. Throughout the session, animals have to increase the number of lever presses to get one reward. The breakpoint is considered the last completed ratio in the session, which is the maximum number of lever presses that a subject is willing to perform to obtain a reinforcer (Richardson and Roberts, 1996; Sharma et al., 2012). Optical stimulation of D2-MSN-VP terminals was given in the cue-exposure period.

During continuous reinforcement (CRF) training (with no stimulation), both D2-ChR2 and D2-YFP groups increased lever pressing throughout days in a similar manner ($p = 0.7246$; Figure 1H). In the fixed-ratio (FR) schedule days, all animals increased lever pressing in the correct versus incorrect lever ($p < 0.0001$; Figure 1I).

After stable lever pressing, animals proceeded to the PR session, in which they received optical stimulation of D2-MSN terminals in the VP paired with the cue light period. D2-MSN-VP stimulation induced a significant increase in the total number of lever presses (D2-ChR2 ON versus OFF; $p = 0.0009$; Figures 1J and S1D). D2-ChR2-stimulated animals increased breakpoint in 57.7% in comparison with D2-YFP-stimulated rats ($p = 0.0014$; Figure 1K). All D2-ChR2 rats showed a significant increase in breakpoint in the session with optical stimulation (ON) in comparison with the session without optical stimulation (OFF) ($p = 0.0234$; Figure 1L). The number of pellets earned was also significantly higher in D2-ChR2 rats in the ON session ($p = 0.031$; Figure S1E). Importantly, lever pressing occurring during the inter-trial interval (ITI) was residual and similar between all groups (~3.5 times less lever presses/min than during trials; Figure S1F). When optogenetic activation occurred during the ITI, no differences were observed between D2-ChR2 and D2-YFP animals (Figures S1G–S1L). D2-YFP animals presented no changes in the session of optical stimulation (ON) in comparison with the session without optical stimulation (OFF), as expected.

These results show that cue-paired optogenetic activation of D2-MSN-VP projections increases motivation.

Optogenetic inhibition of D2-MSN terminals modulates ventral pallidum activity

Next, we performed D2-MSN-VP inhibition experiments using a similar strategy as optical excitation experiment. For the optogenetic inhibition of D2⁺ neurons, we unilaterally injected an AAV5 containing halorhodopsin (NpHR) in fusion with EYFP under the control of the dopamine receptor D2 minimal promoter in the NAc of wild-type rats (D2-NpHR group; Figure 2A). Controls were injected with an adeno-associated virus (AAV) containing EYFP (D2-YFP). We next evaluated optically evoked response of VP neurons to D2-MSN terminal inhibition (589 nm, 4 s of constant light, and 10 mW of light at the tip of the implanted fiber) using single-cell *in vivo* electrophysiology in anesthetized rats (Figure 2A). Thirty-one percent of VP-recorded neurons decreased firing rate, 20.7% increased firing rate, and 48.3% presented no change in comparison with baseline (Figure 2B). The net firing rate (all neurons) of VP did not change during stimulation in comparison with baseline activity (Figure 2C). However, by separating neurons into those that increase or decrease activity to stimulation, a significant effect was observed (p value refers to comparison before stimulation and during stimulation; increase activity,

(H and I) CRF training sessions (H) and FR training sessions (I), showing no differences between groups.

(J) Total number of lever presses in the PR session with optical stimulation of D2-MSN-VP inputs during cue period.

(K and L) Increased breakpoint in the PR session of D2-ChR2 animals in comparison with D2-YFP. $n_{D2-CHR2} = 10$; $n_{D2-YFP} = 9$.

Error bars denote SEM. * $p \leq 0.05$; ** $p \leq 0.01$; *** $p \leq 0.001$. See also Figure S1 and Table S1.

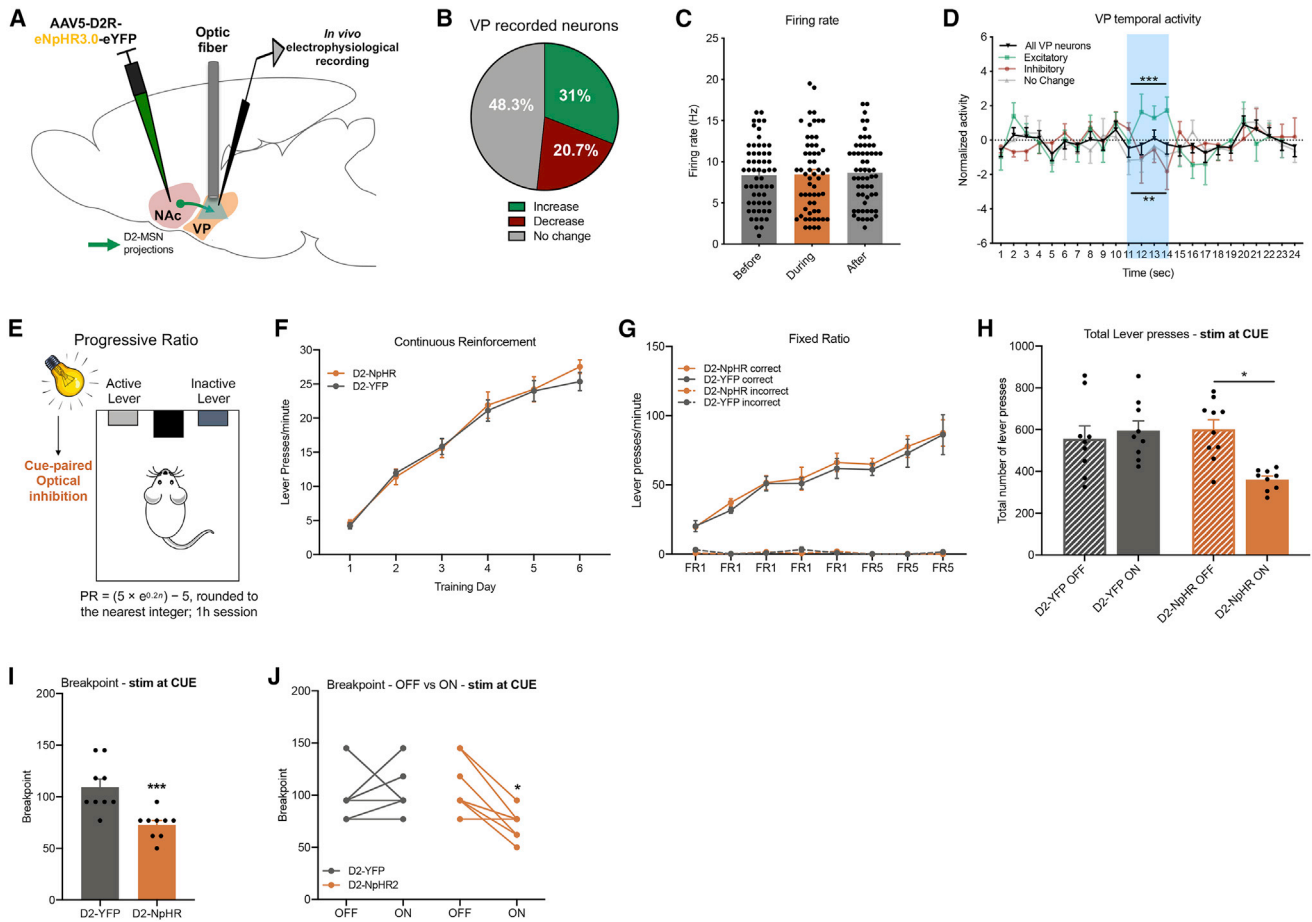


Figure 2. Optogenetic inhibition of D2-MSN-VP terminals during cue exposure decreases motivation

(A) Strategy used for optogenetic inhibition of D2-MSN-VP terminals and electrophysiological recordings in the VP.

(B) Pie chart of VP neurons responding to D2-MSN optical inhibition (589 nm, 4 s of constant light).

(C) VP firing rate ($n = 58$ neurons/4 rats).

(D) PSTH of temporal variation of the normalized activity of VP neurons that increase (green; $n = 18$ neurons), decrease (red; $n = 12$ neurons), and do not change activity (gray; $n = 28$ neurons) during the stimulation period (blue).

(E) Schematic representation of the PR session with optogenetic inhibition of D2-MSN-VP (4 s of constant light at 10 mW) at cue light presentation.

(F and G) CRF training sessions (F) and FR training sessions (G), showing no differences between groups.

(H) Total number of lever presses in the PR session with optical inhibition of D2-MSN-VP inputs during cue period.

(I and J) Decreased breakpoint in the PR session of D2-NpHR animals in comparison with D2-YFP group. $n_{D2-NpHR} = 10$; $n_{D2-YFP} = 9$.

Error bars denote SEM. * $p \leq 0.05$; ** $p \leq 0.01$; *** $p \leq 0.001$. See also [Figure S2](#) and [Table S1](#).

$p = 0.0004$; decrease activity, $p = 0.0059$; no change in activity; [Figure 2D](#)).

Cue-paired optogenetic inhibition of D2-MSN-VP projections decreases motivation

We next performed the training for the PR test. D2-NpHR and D2-YFP rats presented a similar rate of lever pressing in the training sessions. During CRF training, both groups increased lever pressing similarly across days of training ($p = 0.6837$; [Figure 2F](#)), and all animals increased lever pressing in the FR schedule in the correct versus incorrect lever ($p < 0.0001$; [Figure 2G](#)). D2-MSN-VP optical inhibition (589 nm, 4 s of constant light, and 10 mW of light at the tip of the implanted fiber) during cue light period of the PR session induced a significant decrease

in the total number of lever presses (D2-NpHR ON versus OFF; $p = 0.0448$; [Figures 2H](#) and [S2A](#)). This was translated into a 33.5% decrease of the breakpoint of D2-NpHR group in comparison with D2-YFP-stimulated rats ($p = 0.0009$; [Figure 2I](#)). All D2-NpHR rats displayed a significant decrease in breakpoint in the ON session in comparison with the OFF session ($p = 0.0106$; [Figure 2J](#)). D2-NpHR rats earned less pellets in the ON session comparing with the OFF session, though not statistically significant ($p = 0.0653$; [Figure S2B](#)). Lever pressing during the ITI was residual and similar between groups ([Figure S2C](#)). Optogenetic inhibition of D2-MSN-VP inputs during the ITI did not induce differences in the breakpoint ([Figures S2D–S2I](#)).

These results support that cue-paired optogenetic inhibition of D2-MSN-VP projections decreases motivation.

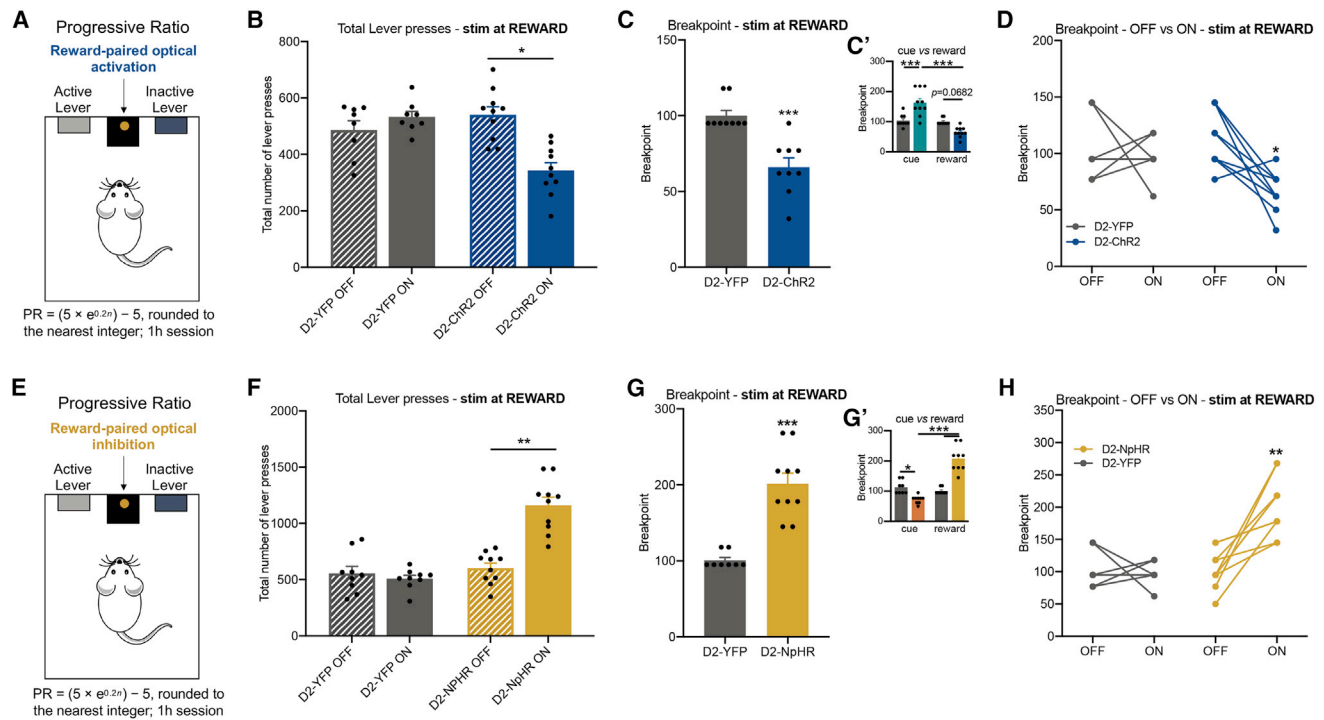


Figure 3. Optogenetic modulation of D2-MSN-VP terminals at reward delivery decreases motivation

(A) Rats were tested in a PR session with optogenetic activation paired with reward delivery. (B) Total number of lever presses in the PR session, showing reduced lever pressing in D2-ChR2 animals in the ON versus OFF session. (C and D) Breakpoint in the PR sessions, showing decreased motivation of D2-ChR2 animals; (C') breakpoint in the PR sessions with optical stimulation at cue exposure and reward delivery is shown. (E) Another group of rats was tested in a PR session with optogenetic inhibition of D2-MSN-VP inputs paired with reward delivery. (F) Total number of lever presses in the PR session, showing increased lever pressing in D2-NpHR animals in the ON versus OFF session. (G and H) Increased breakpoint in the PR session of D2-NpHR animals in comparison with D2-YFP group, when D2-MSN-VP stimulation occurs at reward delivery; (G') breakpoint in the PR sessions with optical inhibition at cue exposure and reward delivery is shown. $n_{D2-ChR2} = 10$; $n_{D2-NpHR} = 10$; $n_{D2-YFP} = 9$. Error bars denote SEM. $^{*}p < 0.01$; $^{**}p \leq 0.01$; $^{***}p \leq 0.001$. See also Figure S3 and Table S1.

Optogenetic modulation of D2-MSN-VP projections during reward delivery alters motivation in the PR test

Since there is some evidence that D2-MSNs activity changes throughout different stages of reward-related behaviors (Calipari et al., 2016; Lafferty et al., 2020; Natsubori et al., 2017), we decided to pair D2-MSN-VP projection activation and inhibition with reward (pellet) delivery (Figures 3A and 3E) during the PR test. Contrary to the effects of optical stimulation during the cue period, D2-ChR2 animals presented a reduced number of total lever presses in the PR session with optical stimulation paired with reward delivery, in comparison with D2-YFP animals (29.4% less; D2-ChR2 reward versus D2-YFP reward: $p = 0.0305$; Figures 3B and S3A). In comparison with D2-YFP, D2-ChR2 presented a 34% reduction in breakpoint ($p = 0.0003$; Figures 3C and 3D). In addition, D2-ChR2 animals presented a significantly lower breakpoint in comparison with the PR session in which they received optical activation paired with cue light exposure ($p = 0.0004$; Figure 3C'). The number of food pellets earned by D2-ChR2 rats in the ON session in comparison with the OFF session was significantly lower ($p = 0.0370$; Figure S3B). The number of lever presses occurring during ITI was similar between groups (Figure S3C).

In another group of animals, we optically inhibited D2-MSN-VP inputs during reward delivery. Optical inhibition paired with reward delivery significantly increased the number of total lever presses in comparison with D2-YFP (128% increase; $p = 0.0005$; Figures 3F and S3D). As compared with D2-YFP, there was a 100.1% increase in breakpoint ($p < 0.0001$; Figure 3G). Plus, D2-NpHR animals presented a significantly higher breakpoint in comparison with the PR session in which they received optical inhibition paired with cue-light exposure ($p < 0.0001$; Figure 3G'). There was also a significant increase in the breakpoint in the ON session in comparison with the OFF session ($p = 0.0035$; Figure 3H). The number of food pellets earned by D2-NpHR rats in the ON session was significantly higher ($p = 0.0048$; Figure S3E). The number of lever presses occurring during ITI was similar between groups (Figure S3F).

These results show that D2-MSN-VP modulation in different stages of the PR test can lead to distinct outcomes: increased activity of D2-MSN-VP projections during the cue period enhances motivation while activation during reward delivery leads to reduced motivation and vice versa for D2-MSN-VP inhibition.

Optogenetic activation of D2-MSN-VP projections paired with reward decreases preference

Considering the previous results suggesting a different role of D2-MSN-VP projections in different stages of the PR test, we evaluated animals in a two-lever, free-choice behavioral paradigm (Robinson et al., 2014). In this task, animals have available two levers that deliver one food pellet each; however, one lever is randomly assigned to optically stimulate D2-MSN-VP projections (stim+), while the other lever is assigned to deliver the pellet alone (stim–; Figure 4A). Throughout the session, animals can press either lever *ad libitum*; pressing one lever in one trial does not exclude the possibility of pressing the other lever in the following trial.

Through the acquisition days, D2-ChR2 rats showed a clear preference for pressing the stim– lever in comparison with the stim+ lever ($p < 0.0001$; Figure 4B), which resulted in receiving significantly more pellet rewards in comparison with pellet + laser rewards (Figure S4A). As expected, D2-YFP rats showed no preference for either lever (Figure 4B). No significant differences were found in the total number of lever presses (in both levers) in the last day of training between D2-ChR2 and D2-YFP rats.

We next decided to evaluate individuals' behavior under reward-extinction conditions (no pellet was delivered on either lever) to verify whether D2-MSN-VP stimulation per se was able to modify behavior (Figure 4D). Interestingly, both groups decreased lever pressing in both levers, indicating that the instrumental response was dependent on the delivery of the reward (Figures 4E and S4C).

After two reminder sessions (similar to acquisition phase), the task was again performed under laser-extinction conditions (pellet delivery in both levers and no laser stimulation; Figure 4G). D2-ChR2 animals showed no preference for either lever under laser-extinction conditions, similarly to D2-YFP animals (Figures 4H and S4E).

Altogether, these data further confirm that optogenetic activation of D2-MSN-VP projections paired with reward reduces preference.

Optogenetic inhibition of D2-MSN-VP projections paired with reward enhances preference

In another set of animals, rats performed the two-lever, free-choice behavioral paradigm with optogenetic inhibition of D2-MSN-VP terminals. Rats were presented with two levers that originated a food pellet, but stim+ was associated with optogenetic inhibition of D2-MSN-VP projections. D2-NpHR rats showed a significant preference for pressing the stim+ lever in comparison with stim– lever ($p < 0.0001$; Figure 4C), resulting in receiving significantly more pellet + laser rewards in comparison with pellet alone (Figure S4B). As anticipated, D2-YFP rats showed no preference for either lever (Figure 4C). No significant differences were found in the total number of lever presses in the last day of training between D2-NpHR and D2-YFP.

We next performed the task under food-extinction conditions (Figure 4D). Both groups significantly decreased lever pressing on either lever (Figures 4F and S4D), indicating that stimulation alone is not sufficient to maintain increased lever pressing.

Thereafter, we performed the same task under laser extinction, which makes the outcome (pellet) equal in both levers (Figure 4G). D2-NpHR animals showed no preference for either lever ($p = 0.001$; Bonferroni multiple comparison, $p > 0.9999$; Figures 4I and S4F).

These data show that optical inhibition paired with reward delivery increases preference in comparison with reward delivery alone.

No differences in food consumption with D2-MSN-VP modulation

In order to verify whether D2-MSN-VP projections play a relevant role in food consumption, we measured the amount of normal chow and food pellets that animals consumed in one session with no optogenetic modulation and one session with either optogenetic activation (D2-ChR2) or optogenetic inhibition (D2-NpHR) of D2-MSN-VP projections (experimental design in Figure S5). For this, all animals performed 3 days of free food consumption and the amount of food consumed was weighted at the end of each 30-min session. Neither optogenetic activation nor optogenetic inhibition of D2-MSN-VP projections had a significant impact on the consumption of normal chow or food pellets (Figure S6), suggesting the absence of differences in food consumption or satiety.

DISCUSSION

Despite remarkable advances in identifying the role of specific neuronal populations of the reward circuit in motivated behaviors (Engelhard et al., 2019; Parker et al., 2016; Saunders et al., 2018), there is still a lot of controversy regarding the role of NAc D1- and D2-MSNs. D2-MSNs have been shown to induce transient punishment and aversive responses and attenuate cocaine conditioning (Bock et al., 2013; Kravitz et al., 2012; Lobo et al., 2010); however, evidence from our team (Soares-Cunha et al., 2016b, 2018, 2020) and others (Cole et al., 2018; Natsubori et al., 2017) points to a heterogeneous role of this neuronal population in behavior. Here, we provide evidence suggesting that D2-MSN terminals in the VP are differentially activated during different phases of motivated behaviors.

In previous studies, we have shown that cue-paired optogenetic activation of D2-MSNs in the NAc significantly increases motivation (Soares-Cunha et al., 2016b). However, others showed that chronic inhibition of these neurons using chemogenetics either increases motivation (Carvalho Poyraz et al., 2016; Gallo et al., 2018) or it has no significant effect (Bock et al., 2013) in motivational levels as measured by the breakpoint in a PR test. These apparently contradictory findings can now be reconciled with the evidence showing that D2-MSNs play distinct roles during different stages of reward-related tasks, which potentially explain the divergent results between optogenetics (acute manipulation) and designer receptors exclusively activated by designer drugs (DREADD) (chronic manipulation) experiments. Moreover, it was shown that distinct patterns of optical activation of D1- and D2-MSNs can lead to place preference or avoidance (Soares-Cunha et al., 2020).

The data presented in this work indicate that D2-MSN-VP projections are important to add value to a cue that predicts a future

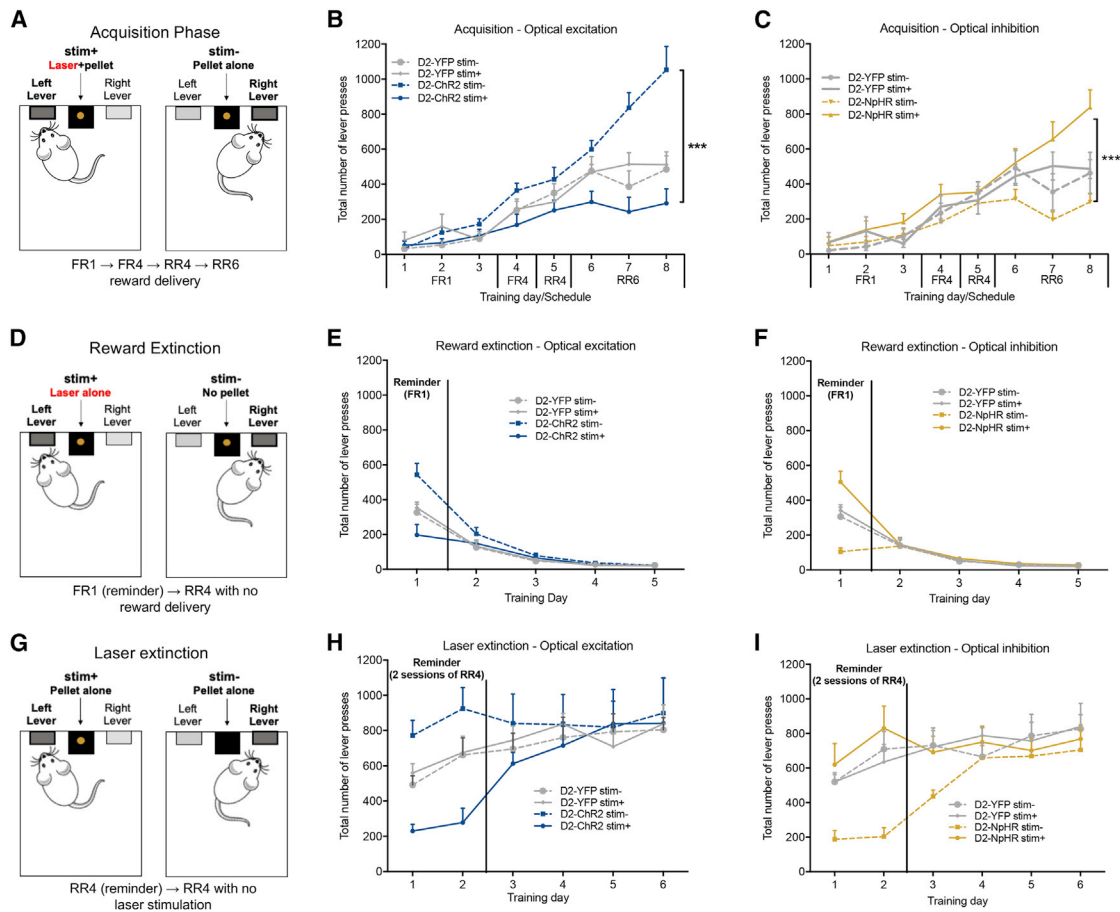


Figure 4. Optical activation and inhibition of D2-MSN-VP terminals paired with reward delivery reduces and increases preference

(A) Two-choice acquisition lever pressing task: pressing stim+ lever results in the delivery of a food pellet reward and optical stimulation or inhibition; pressing stim- lever results in delivery of food pellet reward alone.
 (B) Lever press acquisition phase for D2-ChR2 and D2-YFP rats.
 (C) Lever press acquisition phase for D2-NpHR and D2-YFP rats.
 (D) Under pellet-extinction sessions, no reward is given in any of the levers.
 (E) Pellet-extinction session of D2-ChR2 and D2-YFP rats.
 (F) Pellet-extinction session of D2-NpHR and D2-YFP rats.
 (G) Laser-extinction sessions where no stimulation is given.
 (H) Laser-extinction session of D2-ChR2 and D2-YFP rats.
 (I) Laser-extinction sessions of D2-NpHR and D2-YFP rats. $n_{D2-ChR2} = 7$; $n_{D2-NpHR} = 5$; $n_{D2-YFP} = 6$.
 Error bars denote SEM. *** $p \leq 0.001$. See also [Figure S4](#) and [Table S1](#).

reward and increase effort towards obtaining the reward. Conversely, suppression of D2-MSN-VP activity is required for efficient reward consumption. In agreement, in the two-choice task, optogenetic activation of D2-MSN-VP projections resulted in decreased preference for the lever that resulted in laser stimulation + reward delivery (stim+), in comparison with the lever that resulted in the delivery of the pellet alone (stim-); the contrary was observed with optical inhibition of these terminals.

In line with our data, electrophysiological studies showed that NAc MSNs exhibit phasic increases in firing rate during cue presentations but attenuated firing rates at reward delivery ([Am-broggi et al., 2011](#); [Day et al., 2011](#); [Gale et al., 2014](#); [Roitman et al., 2005](#)). Similarly, electrophysiological recordings during a Pavlovian conditioning task showed that MSNs exhibit signifi-

cant responses during task performance: while MSNs increase firing rate during the conditioned stimulus, the responses to reward were predominantly inhibitory ([Day and Carelli, 2007](#); [Wan and Peoples, 2006](#)). Yet, it is important to mention that, in these studies, no segregation between D1- and D2-MSNs was done due to technical limitations. More recently, a key role for NAc D2-MSNs in response to reward-predicting cue was identified, such that these neurons increased firing at cue that predicted lever availability for electrical stimulation of the VTA, while at lever pressing, it was mainly D1-MSNs ([Owesson-White et al., 2016](#)). Interestingly, calcium transients of D1- or D2-MSNs in the ventrolateral striatum during a PR task showed that D2-MSNs increase activity at trial start but decrease as lever pressing for reward continues, reaching minimal levels at reward delivery

(Natsubori et al., 2017). Also, higher D2-MSN calcium transients associated with cue exposure were correlated with a higher motivational state (Natsubori et al., 2017). Although ventrolateral striatum is functionally distinct from the NAc, these data are in agreement with our results indicating that D2-MSN activity in the NAc is highly relevant for the reward-predicting cue period.

One possible explanation for the observed motivation enhancement is that D2-MSNs could play an important role in discrimination learning, refining learned reinforced behavior (Iino et al., 2020; Lee et al., 2021). Activation of D2-MSN-VP projections can also induce an indirect effect in downstream regions important for motivation, namely the VTA, that is innervated by the VP (Hjelmstad et al., 2013; Ostlund et al., 2014; Soares-Cunha et al., 2018, 2020). In agreement, previous data from our team showed that optical activation of D2-MSNs leads to inhibition of VP GABAergic neurons and consequent increase in VTA dopamine neuronal activity (Soares-Cunha et al., 2018, 2020). Dopaminergic signals arising from the VTA in the NAc can signal a reward prediction error (RPE), encoding the difference between actual and predicted reward (Hart et al., 2014; Sadoris et al., 2015; Schultz et al., 1997), crucial for reinforcement learning. As learning progresses, this dopamine signal is transferred from the reward to cues that signal reward availability (Roitman, 2004). Thus, it is tempting to speculate that the dopamine increase during the cue period elicited by D2-MSN-VP stimulation invigorates the behavioral response to obtain the reward, leading to increased breakpoint. Interestingly, ~30% of VP neurons can encode RPEs (Otenheimer et al., 2020), so one may also speculate that increasing D2-MSN GABAergic tone to the VP during reward delivery might mimic a negative RPE signal that reduces motivation.

We also found that, under reward extinction, laser stimulation per se was not able to support the shift in preference. These data may be difficult to reconcile with the fact that brief optical activation of D2-MSNs induces place preference (Cole et al., 2018; Soares-Cunha et al., 2020). Still, these findings are similar to previous studies in which optogenetic stimulation of central amygdala and laterodorsal tegmentum-to-NAc projections only increased preference for the lever associated with optical stimulation if paired with reward (Coimbra et al., 2019; Robinson et al., 2014). One possible explanation is that, in the two-choice task, animals are mildly food restricted so their primary goal is to obtain food, so under reward extinction, stimulation alone is not enough to sustain lever pressing. Another possibility is that one would need additional sessions or different stimulation parameters to observe self-stimulation of D2-MSN-VP inputs, especially considering the importance of the pattern of activity of D2-MSNs in valence-related behaviors (Soares-Cunha et al., 2020).

In conclusion, we show that D2-MSN-VP projections differentially contribute to distinct phases of motivated behavior: activity of these neurons is necessary for the invigorating value of a cue that predicts a reward but is not as relevant for the operant execution of the task or for the consumption of the reward. Altogether, this study contributes to the growing body of evidence showing that D2-MSNs are not necessarily “aversive,” exhibiting a complex role in motivated behaviors, and that additional studies are needed to fully disclose their role in behavior.

Limitations of the study

Our study has some limitations that are important to pinpoint. One obvious limitation is the inclusion of only males in the experiments, though previous data from our laboratory suggest that there are no major differences between sexes in the tasks that were used. Nevertheless, since there is the possibility of subtle sex differences, females should be included in future studies.

Another caveat is that we optogenetically manipulated D2-MSN-VP inputs during different stages of behavior to mimic endogenous activation and inhibition of these inputs. We have used stimulation protocols that trigger activity changes that resemble *physiological* changes in both the NAc and VP (Soares-Cunha et al., 2016b, 2020); however, it is not possible to determine precisely how close the exogenous pattern of activation and inhibition is to endogenous activation and inhibition. This emphasizes the importance of recording neuronal activity *in vivo* during a motivation-related task, either with large-scale electrophysiological recordings with opto-tagging to allow MSN segregation (Sjulson et al., 2018) or calcium imaging of selected MSNs (Klaus et al., 2017), in order to determine the temporal activity of these neurons during behavior. The possibility of identifying activity changes in individual neurons would be crucial to further comprehend the role of D2-MSNs in behavior.

STAR★METHODS

Detailed methods are provided in the online version of this paper and include the following:

- KEY RESOURCES TABLE
- RESOURCE AVAILABILITY
 - Lead contact
 - Materials availability
 - Data and code availability
- EXPERIMENTAL MODEL AND SUBJECT DETAILS
- METHOD DETAILS
 - Constructs and virus
 - Surgery and optic fiber implantation
 - Behavior
 - Optogenetic manipulation
 - *In vivo* single cell electrophysiological recordings
 - Immunofluorescence
- QUANTIFICATION AND STATISTICAL ANALYSIS

SUPPLEMENTAL INFORMATION

Supplemental information can be found online at <https://doi.org/10.1016/j.celrep.2022.110380>.

ACKNOWLEDGMENTS

We would like to acknowledge Karl Deisseroth from Stanford University for providing the viral constructs. C.S.-C. and B.C. have Scientific Employment Stimulus Contracts from the Portuguese Foundation for Science and Technology (FCT) (CEECIND/03887/2017 and CEECIND/03898/2020). A.V.D. has an FCT grant (SFRH/BD/147066/2019). This work was funded by Bial Foundation grants 30/2016 and 175/20 and by FCT under the scope of the projects PTDC/MED-NEU/29071/2017 (REWSTRESS) and PTDC/MED-NEU/4804/2020 (EN-DOPIO). Part of the work has received funding from “‘la Caixa’” Foundation (ID 100010434), under the agreement LCF/PR/HR20/52400020. This project

has received funding from the European Research Council (ERC) under the European Union's Horizon 2020 research and innovation program (grant agreement no. 101003187). Part of the work was also funded by national funds through the FCT—project UIDB/50026/2020 and UIDP/50026/2020, and by the ICVS Scientific Microscopy Platform, member of the national infrastructure PPBI - Portuguese Platform of Bioimaging (PPBI-POCI-01-0145-FEDER-022122).

AUTHOR CONTRIBUTIONS

C.S.-C. performed and designed experiments, analyzed the data, and wrote the manuscript. A.J.R. and N.S. designed experiments and wrote the manuscript. A.V.D., R.C., N.V.-G., B.C., and L.P. performed experiments. N.A.P.d.V. analyzed data. A.J.R. and C.S.-C. secured funding.

DECLARATION OF INTERESTS

The authors declare no competing interests.

Received: January 9, 2021

Revised: November 6, 2021

Accepted: January 24, 2022

Published: February 15, 2022

REFERENCES

Ambroggi, F., Ghazizadeh, A., Nicola, S.M., and Fields, H.L. (2011). Roles of nucleus accumbens core and shell in incentive-cue responding and behavioral inhibition. *J. Neurosci.* *31*, 6820–6830.

Benazzouz, A., Gao, D.M., Ni, Z.G., Piallat, B., Bouali-Benazzouz, R., and Benabid, A.L. (2000). Effect of high-frequency stimulation of the subthalamic nucleus on the neuronal activities of the substantia nigra pars reticulata and ventrolateral nucleus of the thalamus in the rat. *Neuroscience* *99*, 289–295.

Berridge, K.C. (2012). From prediction error to incentive salience: mesolimbic computation of reward motivation: from prediction error to incentive salience. *Eur. J. Neurosci.* *35*, 1124–1143.

Bock, R., Shin, J.H., Kaplan, A.R., Dobi, A., Markey, E., Kramer, P.F., Gremel, C.M., Christensen, C.H., Adrover, M.F., and Alvarez, V.A. (2013). Strengthening the accumbal indirect pathway promotes resilience to compulsive cocaine use. *Nat. Neurosci.* *16*, 632–638.

Calipari, E.S., Bagot, R.C., Purushothaman, I., Davidson, T.J., Yorgason, J.T., Peña, C.J., Walker, D.M., Pirpinias, S.T., Guise, K.G., Ramakrishnan, C., et al. (2016). *In vivo* imaging identifies temporal signature of D1 and D2 medium spiny neurons in cocaine reward. *Proc. Natl. Acad. Sci. U. S. A.* *113*, 2726–2731.

Carelli, R.M. (2002). Nucleus accumbens cell firing during goal-directed behaviors for cocaine vs. 'natural' reinforcement. *Physiol. Behav.* *76*, 379–387.

Carvalho Poyraz, F., Holzner, E., Bailey, M.R., Meszaros, J., Kenney, L., Kheirbek, M.A., Balsam, P.D., and Kellendonk, C. (2016). Decreasing striatopallidal pathway function enhances motivation by energizing the initiation of goal-directed action. *J. Neurosci.* *36*, 5988–6001.

Chang, S.E., Todd, T.P., and Smith, K.S. (2018). Paradoxical accentuation of motivation following accumbens-pallidum disconnection. *Neurobiol. Learn. Mem.* *149*, 39–45.

Coimbra, B., Soares-Cunha, C., Vasconcelos, N.A.P., Domingues, A.V., Borges, S., Sousa, N., and Rodrigues, A.J. (2019). Role of laterodorsal tegmentum projections to nucleus accumbens in reward-related behaviors. *Nat. Commun.* *10*, 4138.

Cole, S.L., Robinson, M.J.F., and Berridge, K.C. (2018). Optogenetic self-stimulation in the nucleus accumbens: D1 reward versus D2 ambivalence. *PLoS One* *13*, e0207694.

Day, J.J., and Carelli, R.M. (2007). The nucleus accumbens and Pavlovian reward learning. *Neuroscientist* *13*, 148–159.

Day, J.J., Jones, J.L., and Carelli, R.M. (2011). Nucleus accumbens neurons encode predicted and ongoing reward costs in rats: nucleus accumbens and reward cost. *Eur. J. Neurosci.* *33*, 308–321.

Engelhard, B., Finkelstein, J., Cox, J., Fleming, W., Jang, H.J., Ornelas, S., Koay, S.A., Thiberge, S.Y., Daw, N.D., Tank, D.W., et al. (2019). Specialized coding of sensory, motor and cognitive variables in VTA dopamine neurons. *Nature* *570*, 509–513.

Ferguson, L.M., Ahrens, A.M., Longyear, L.G., and Aldridge, J.W. (2020). Neurons of the ventral tegmental area encode individual differences in motivational "wanting" for reward cues. *J. Neurosci.* *40*, 8951–8963.

Gale, J.T., Shields, D.C., Ishizawa, Y., and Eskandar, E.N. (2014). Reward and reinforcement activity in the nucleus accumbens during learning. *Front. Behav. Neurosci.* *8*, 114.

Gallo, E.F., Meszaros, J., Sherman, J.D., Chohan, M.O., Teboul, E., Choi, C.S., Moore, H., Javitch, J.A., and Kellendonk, C. (2018). Accumbens dopamine D2 receptors increase motivation by decreasing inhibitory transmission to the ventral pallidum. *Nat. Commun.* *9*, 1086.

Gerfen, C.R., and Surmeier, D.J. (2011). Modulation of striatal projection systems by dopamine. *Annu. Rev. Neurosci.* *34*, 441–466.

Hart, A.S., Rutledge, R.B., Glimcher, P.W., and Phillips, P.E.M. (2014). Phasic dopamine release in the rat nucleus accumbens symmetrically encodes a reward prediction error term. *J. Neurosci.* *34*, 698–704.

Hjelmstad, G.O., Xia, Y., Margolis, E.B., and Fields, H.L. (2013). Opioid modulation of ventral pallidal afferents to ventral tegmental area neurons. *J. Neurosci.* *33*, 6454–6459.

Iino, Y., Sawada, T., Yamaguchi, K., Tajiri, M., Ishii, S., Kasai, H., and Yagishita, S. (2020). Dopamine D2 receptors in discrimination learning and spine enlargement. *Nature* *579*, 555–560.

Ilango, A., Kesner, A.J., Broker, C.J., Wang, D.V., and Ikemoto, S. (2014). Phasic excitation of ventral tegmental dopamine neurons potentiates the initiation of conditioned approach behavior: parametric and reinforcement-schedule analyses. *Front. Behav. Neurosci.* *8*, 155.

Klaus, A., Martins, G.J., Paixao, V.B., Zhou, P., Paninski, L., and Costa, R.M. (2017). The spatiotemporal organization of the striatum encodes action space. *Neuron* *95*, 1171–1180.e7.

Kravitz, A.V., Tye, L.D., and Kreitzer, A.C. (2012). Distinct roles for direct and indirect pathway striatal neurons in reinforcement. *Nat. Neurosci.* *15*, 816–818.

Kupchik, Y.M., Brown, R.M., Heinsbroek, J.A., Lobo, M.K., Schwartz, D.J., and Kalivas, P.W. (2015). Coding the direct/indirect pathways by D1 and D2 receptors is not valid for accumbens projections. *Nat. Neurosci.* *18*, 1230–1232.

Lafferty, C.K., Yang, A.K., Mendoza, J.A., and Britt, J.P. (2020). Nucleus accumbens cell type- and input-specific suppression of unproductive reward seeking. *Cell Rep.* *30*, 3729–3742.e3.

Lee, S.J., Lodder, B., Chen, Y., Patriarchi, T., Tian, L., and Sabatini, B.L. (2021). Cell-type-specific asynchronous modulation of PKA by dopamine in learning. *Nature* *590*, 451–456.

Lobo, M.K., Covington, H.E., Chaudhury, D., Friedman, A.K., Sun, H., Damez-Werno, D., Dietz, D.M., Zaman, S., Koo, J.W., Kennedy, P.J., et al. (2010). Cell type-specific loss of BDNF signaling mimics optogenetic control of cocaine reward. *Science* *330*, 385–390.

Lu, X.-Y., Behnam Ghasemzadeh, M., and Kalivas, P.W. (1997). Expression of D1 receptor, D2 receptor, substance P and enkephalin messenger RNAs in the neurons projecting from the nucleus accumbens. *Neuroscience* *82*, 767–780.

Mohebi, A., Pettibone, J.R., Hamid, A.A., Wong, J.-M.T., Vinson, L.T., Patriarchi, T., Tian, L., Kennedy, R.T., and Berke, J.D. (2019). Dissociable dopamine dynamics for learning and motivation. *Nature* *570*, 65–70.

Natsubori, A., Tsutsui-Kimura, I., Nishida, H., Boucheikioua, Y., Sekiya, H., Uchigashima, M., Watanabe, M., de Kerchove d'Exaerde, A., Mimura, M., Takata, N., et al. (2017). Ventrolateral striatal medium spiny neurons positively regulate food-incentive, goal-directed behavior independently of D1 and D2 selectivity. *J. Neurosci.* *37*, 2723–2733.

- Nicklas, W., Baneux, P., Boot, R., Decelle, T., Deeny, A.A., Fumanelli, M., and Illgen-Wilcke, B. (2002). Recommendations for the health monitoring of rodent and rabbit colonies in breeding and experimental units. *Lab. Anim.* 36, 20–42.
- Nicola, S.M., Yun, I.A., Wakabayashi, K.T., and Fields, H.L. (2004). Cue-evoked firing of nucleus accumbens neurons encodes motivational significance during a discriminative stimulus task. *J. Neurophysiol.* 91, 1840–1865.
- Ostlund, S.B., LeBlanc, K.H., Kosheleff, A.R., Wassum, K.M., and Maidment, N.T. (2014). Phasic mesolimbic dopamine signaling encodes the facilitation of incentive motivation produced by repeated cocaine exposure. *Neuropsychopharmacology* 39, 2441–2449.
- Ottenheimer, D., Richard, J.M., and Janak, P.H. (2018). Ventral pallidum encodes relative reward value earlier and more robustly than nucleus accumbens. *Nat. Commun.* 9, 4350.
- Ottenheimer, D.J., Bari, B.A., Sutlief, E., Fraser, K.M., Kim, T.H., Richard, J.M., Cohen, J.Y., and Janak, P.H. (2020). A quantitative reward prediction error signal in the ventral pallidum. *Nat. Neurosci.* 23, 1267–1276.
- Owesson-White, C., Belle, A.M., Herr, N.R., Peele, J.L., Gowrishankar, P., Carelli, R.M., and Wightman, R.M. (2016). Cue-evoked dopamine release rapidly modulates D2 neurons in the nucleus accumbens during motivated behavior. *J. Neurosci.* 36, 6011–6021.
- Parker, N.F., Cameron, C.M., Taliaferro, J.P., Lee, J., Choi, J.Y., Davidson, T.J., Daw, N.D., and Witten, I.B. (2016). Reward and choice encoding in terminals of midbrain dopamine neurons depends on striatal target. *Nat. Neurosci.* 19, 845–854.
- Paxinos, G., and Watson, C. (2005). *The Rat Brain in Stereotaxic Coordinates* (New York: Academic Press).
- Richard, J.M., Ambroggi, F., Janak, P.H., and Fields, H.L. (2016). Ventral pallidum neurons encode incentive value and promote cue-elicited instrumental actions. *Neuron* 90, 1165–1173.
- Richardson, N.R., and Roberts, D.C.S. (1996). Progressive ratio schedules in drug self-administration studies in rats: a method to evaluate reinforcing efficacy. *J. Neurosci. Methods* 66, 1–11.
- Robinson, M.J.F., Warlow, S.M., and Berridge, K.C. (2014). Optogenetic excitation of central amygdala amplifies and narrows incentive motivation to pursue one reward above another. *J. Neurosci.* 34, 16567–16580.
- Roitman, M.F. (2004). Dopamine operates as a subsecond modulator of food seeking. *J. Neurosci.* 24, 1265–1271.
- Roitman, M.F., Wheeler, R.A., and Carelli, R.M. (2005). Nucleus accumbens neurons are innately tuned for rewarding and aversive taste stimuli, encode their predictors, and are linked to motor output. *Neuron* 45, 587–597.
- Saddoris, M.P., Cacciapaglia, F., Wightman, R.M., and Carelli, R.M. (2015). Differential dopamine release dynamics in the nucleus accumbens core and shell reveal complementary signals for error prediction and incentive motivation. *J. Neurosci.* 35, 11572–11582.
- Saunders, B.T., Richard, J.M., Margolis, E.B., and Janak, P.H. (2018). Dopamine neurons create Pavlovian conditioned stimuli with circuit-defined motivational properties. *Nat. Neurosci.* 21, 1072–1083.
- Schultz, W., Dayan, P., and Montague, P.R. (1997). A neural substrate of prediction and reward. *Science* 275, 1593–1599.
- Sharma, S., Hryhorczuk, C., and Fulton, S. (2012). Progressive-ratio responding for palatable high-fat and high-sugar food in mice. *J. Vis. Exp.*, e3754.
- Sjulson, L., Peyrache, A., Cumpelik, A., Cassataro, D., and Buzsáki, G. (2018). Cocaine place conditioning strengthens location-specific hippocampal coupling to the nucleus accumbens. *Neuron* 98, 926–934.e5.
- Soares-Cunha, C., Coimbra, B., Sousa, N., and Rodrigues, A.J. (2016a). Reappraising striatal D1- and D2-neurons in reward and aversion. *Neurosci. Biobehav. Rev.* 68, 370–386.
- Soares-Cunha, C., Coimbra, B., David-Pereira, A., Borges, S., Pinto, L., Costa, P., Sousa, N., and Rodrigues, A.J. (2016b). Activation of D2 dopamine receptor-expressing neurons in the nucleus accumbens increases motivation. *Nat. Commun.* 7, 11829.
- Soares-Cunha, C., Coimbra, B., Domingues, A.V., Vasconcelos, N., Sousa, N., and Rodrigues, A.J. (2018). Nucleus accumbens microcircuit underlying D2-MSN-driven increase in motivation. *eNeuro* 5, ENEURO.0386-18.2018.
- Soares-Cunha, C., de Vasconcelos, N.A.P., Coimbra, B., Domingues, A.V., Silva, J.M., Loureiro-Campos, E., Gaspar, R., Sotiropoulos, I., Sousa, N., and Rodrigues, A.J. (2020). Nucleus accumbens medium spiny neurons subtypes signal both reward and aversion. *Mol. Psychiatry* 25, 3241–3255.
- Wan, X., and Peoples, L.L. (2006). Firing patterns of accumbal neurons during a Pavlovian-conditioned approach task. *J. Neurophysiol.* 96, 652–660.
- Zalocusky, K.A., Ramakrishnan, C., Lerner, T.N., Davidson, T.J., Knutson, B., and Deisseroth, K. (2016). Nucleus accumbens D2R cells signal prior outcomes and control risky decision-making. *Nature* 537, 642–646.

STAR★METHODS

KEY RESOURCES TABLE

REAGENT or RESOURCE	SOURCE	IDENTIFIER
Antibodies		
Mouse polyclonal anti-DR2	Santa Cruz Biotechnology	catalog #sc-5303, RRID: AB_668816
Goat polyclonal anti-GFP	Abcam	catalog #A-11055, RRID: AB_2534102
Alexa fluor 488 donkey anti-goat	Thermo Fisher Scientific	catalog #A-11055, RRID: AB_2534102
Alexa fluor 594 donkey anti-mouse	Thermo Fisher Scientific	catalog #A-21203, RRID: AB_141633
DAPI (4',6-Diamidino-2-Phenylindole, Dihydrochloride)	Thermo Fisher Scientific	catalog #1306, RRID: AB_2629482
Bacterial and virus strains		
AAV5-D2R-hChR2(H134R)-EYFP	Karl Deisseroth lab	N/A link lab
AAV5-D2R-eNpHR3.0-EYFP	Karl Deisseroth lab	N/A
AAV5-D2R- EYFP	Karl Deisseroth lab	N/A
Experimental models: Organisms/strains		
<i>Ratus norvegicus</i> , Wistar han IGS rats	Charles River Laboratories, Spain	Strain #273
Software and algorithms		
Spike2	Cambridge Electronic Design	RRID: SCR_000903 https://ced.co.uk/downloads/latestsoftware
Med-PC program	Med Associates	RRID: SCR_012156 https://www.med-associates.com/med-pc-v/
GraphPad Prism	GraphPad Software Inc	RRID: SCR_002798 https://www.graphpad.com/scientific-software/prism/

RESOURCE AVAILABILITY

Lead contact

Further information and requests for resources and reagents should be directed to and will be fulfilled by the Lead Contact, Dr. Ana João Rodrigues (ajrodrigues@med.uminho.pt).

Materials availability

This study did not generate new unique reagents.

Data and code availability

- All data reported in this paper will be shared by the lead contact upon request.
- This paper does not report original code.
- Any additional information required to reanalyze the data reported in this paper is available from the lead contact upon request.

EXPERIMENTAL MODEL AND SUBJECT DETAILS

Male *Wistar Han* IGS rats (Charles River Laboratories, strain #273) with two to three months of age at the beginning of the experiments were used. Animals were maintained under standard housing conditions with 12/12h light/dark cycle (lights on from 8a.m. to 8p.m.) and room temperature of $21 \pm 1^\circ\text{C}$, with relative humidity of 50–60%. Rats were individually housed after optical fiber implantation and standard diet (4RF21, Mucedola SRL) and water were given *ad libitum*, until the beginning of the behavioral experiments, in which animals switched to food restriction to maintain 85% of initial body weight.

Behavioral manipulations occurred during the light period of the light/dark cycle. Health monitoring was performed according to FELASA guidelines (Nicklas et al., 2002). All procedures were conducted in accordance with European Regulations (European Union Directive 2010/63/EU). Animal facilities and animal experimenters were certified by the National regulatory entity, Direção-Geral de

Alimentação e Veterinária (DGAV). All protocols were approved by the Ethics Committee of the Life and Health Sciences Research Institute (ICVS) and by DGAV (protocol number 19074, approved on 08/30/2016).

Group I of animals performed the progressive ratio schedule of reinforcement, with optical stimulation at cue, at reward, or during the ITI (Figures 1, 2, and 3).

Group II of animals performed the two-choice schedule of reinforcement (Figure 4) and the food consumption test (Figures S5 and S6).

METHOD DETAILS

Constructs and virus

eYFP or hChr2(H134R)-eYFP or eNpHR3.0-eYFP were cloned under the control of the D2R minimal promoter region as described before (Soares-Cunha et al., 2016b; Zalocusky et al., 2016). Constructs were packaged in AAV5 serotype by the University of North Carolina at Chapel Hill (UNC) Gene Therapy Center Vector Core. AAV5 vector titers were $3.7\text{--}6 \times 10^{12}$ viral molecules/ml as determined by dot blot.

Surgery and optic fiber implantation

Rats were anesthetized with 75 mg kg^{-1} ketamine (Imalgene, Merial) plus 0.5 mg kg^{-1} medetomidine (Dorbene, Cymedica). Virus was unilaterally injected into the NAc; coordinates from bregma, according to (Paxinos and Watson, 2005): +1.2 mm anteroposterior (AP), +1.2 mm mediolateral (ML), and -6.5 mm dorsoventral (DV; D2-ChR2 group, D2-NpHR group and D2-YFP control group). An optic fiber was then implanted in the VP (coordinates from bregma: -0.1 mm AP, +2.4 mm ML, and -7.5 mm DV), which was secured to the skull using two 2.4 mm screws (Bilaney) and dental cement (C&B kit, Sun Medical).

Rats were allowed to recover for three weeks before initiation of the behavioral trainings.

Behavior

Animals and apparatus

Male Wistar han rats (2–3 months old at the beginning of the experiments) were habituated to 45 mg food pellets (F0021; Bio-Serve) in the home cage, which were used as reward during the behavioral protocol, 3 days before training initiation. Behavioral sessions were performed in operant chambers (Med Associates) that contained a central, recessed magazine to provide access to 45 mg food pellets (Bio-Serve), two retractable levers with cue lights located above them that were located on each side of the magazine. Chamber illumination was obtained through a 2.8-W, 100-mA light, positioned at the top-center of the wall opposite to the magazine. The chambers were controlled by a computer equipped with the Med-PC software (Med Associates).

Progressive ratio schedule of reinforcement (PR)

This behavioral protocol was adapted from a previously-described PR test for mice using food pellets as reward (Sharma et al., 2012), applying a classical schedule of reinforcement (Richardson and Roberts, 1996).

Operant training started with a continuous reinforcement (CRF) schedule with one lever extended with no cue light being present; the lever would remain extended throughout the session, and a single lever press would deliver a food pellet (maximum of 50 pellets earned within 30 minutes). In the first sessions, food pellet dust was placed on the lever to promote lever pressing. Rats were trained to lever press on the opposite lever, in a second CRF session performed in the same day, using the same training procedure. In the four following days, the side of the correct lever was alternated between sessions. After successful completion of the CRF training (6 days), rats were trained to lever press one time for a single food pellet in a fixed ratio (FR) schedule consisting in 50 trials in which both levers are presented, but the correct lever is signaled by the illumination of a cue light above it. FR sessions began with extension of both levers (correct and incorrect) and illumination of the house light and the cue light over the correct lever. Completion of the correct number of lever presses led to a pellet delivery, followed by a 30 second inter-trial interval (ITI). During ITI, the cue light above the correct lever and the house light were turned OFF, and additional lever-pressing was registered but did not result in the delivery of a food pellet. This ITI period allows time for rats to consume the food pellet and return to *baseline behavior*. Assignment of the correct lever was counterbalanced within each group. Each FR1 training session lasted 1 hour or when 50 pellets have been delivered. In a similar manner, rats were then trained using an FR5 reinforcement schedule.

The rats were then trained in the progressive ratio (PR) schedule of reinforcement. The response ratio schedule during PR test was calculated according to Richardson and Roberts (1996) using the following mathematical formula (rounded to the nearest integer): $= [5e^{(R^{0.2})}] - 5$ where R is the number of food rewards already earned plus 1. Thus, the number of responses required to earn a food reward follow the order: 1, 2, 4, 6, 9, 12, 15, 20, 25, 32, 40, 50, 62, 77, 95, 118, 145 and so on. Failure to press the lever in any 10-minute period resulted in termination of the session. None of the animals failed to press in any 10 min period of the task, so in all of the animals the session lasted 1h. During PR sessions, a 30-second ITI was also applied. During this period, the house light and cue lights were turned OFF but levers were not retracted. Lever pressing during ITI was registered but was not accounted for PR schedule progression. The last completed ratio was set as the breakpoint (Richardson and Roberts, 1996).

Each rat performed 4 sessions of PR: in the first session all animals received no optogenetic manipulation; in following sessions, one third of the animals received optogenetic manipulation during ITI, one third received optogenetic manipulation at cue exposure and one third received optogenetic manipulation at pellet delivered. The days of optogenetic manipulation were counterbalanced between groups.

At the end of the sessions, data was registered and total number of lever presses during trials, number of food pellets earned, breakpoint (the last completed ratio) and the total number of lever presses performed during ITI were obtained.

Optical activation consisted of: 473nm, 1s at 20Hz, 20 light pulses of 25ms, 50% duty cycle, 10mW at the tip of the implanted fiber.

Optical inhibition consisted of: 589nm, 4s of constant light, 10mW at the tip of the implanted fiber.

Two-choice schedule of reinforcement

This behavioral protocol was adapted from the one previously described by (Robinson et al., 2014).

Acquisition phase. During instrumental training, rats were presented two levers signaled by the illumination of a cue light above it, one on either side of the magazine. Presses in one lever (stim+: laser + pellet) lead to delivery of a pellet plus laser stimulation (optical activation: 473nm, 1s at 20Hz, 20 light pulses of 25ms, 50% duty cycle; optical inhibition: 589 nm, 4s constant light; both with 10mW at the tip of the implanted fiber) accompanied by a 4s auditory cue (white noise or tone; always the same paired with this outcome for a particular rat, but counterbalanced assignments across rats). In contrast, pressing the other lever (stim-: pellet alone) delivered a single pellet accompanied by another 4s auditory cue (tone or white noise), but with no laser stimulation. For both levers, presses during the 4s after pellet delivery had no further consequence. After 2 d of initial acquisition, each daily session began with a single lever presented alone to allow opportunity to earn its associated reward (either stim+ (laser+pellet) or stim- (pellet alone) - forced trials), after which the lever was retracted. Then, the alternative lever was presented alone to allow opportunity to earn the other reward. Each lever was presented again alone for a second cycle to ensure sampling of both reward outcomes. The forced choice exposures were intended to allow the rat to better acquire the association between each lever and its specific outcome. Finally, both levers were extended together for the remainder of the session (30 min total), allowing the rat to freely choose between the two levers and to earn respective rewards in any ratio it chose. Whenever the number of lever presses required by a day's schedule was completed on either lever (FR1, FR4, RR4, RR6), a pellet was immediately delivered, accompanied by 4 s of the assigned auditory cue for the particular lever and its outcome (white noise or tone). For the stim+ lever, delivery of the pellet was also accompanied by additional simultaneous laser stimulation (optical activation: 473nm, 1s at 20Hz, 20 light pulses of 25ms, 50% duty cycle; optical inhibition: 589 nm, 4s constant light). During the 4s, animals rapidly retrieved the food pellet and then resumed responding on either of the two levers.

All animals were trained on the following increasing schedule of responding effort: fixed ratio (FR) 1 (1 lever press resulted in 1 reward delivery), one day of FR4 (4 lever presses resulted in 1 reward delivery), one day of random ratio (RR) 4 (probability of delivery of 1 reward at every 4 lever presses) and three days of RR6 (probability of delivery of 1 reward at every 6 lever presses). At the end of the session total number of lever presses on the stim+ and stim-, as well as the number of rewards received were collected and plotted.

Food extinction phase. To assess whether laser stimulation alone could maintain responding on the stim+ associated lever when the food pellet was discontinued, rats were given the opportunity to press in both levers but without pellet (pellet extinction). This closely corresponds to a form of laser self-stimulation test, but using an already established instrumental response that had been learned to earn laser+pellet (stim+) or pellet alone (stim-) combinations. Each completed trial (RR4) on the stim+ (previously laser+pellet) lever resulted in the delivery of laser stimulation (optical activation: 473nm, 1s at 20Hz, 20 light pulses of 25ms, 50% duty cycle; optical inhibition: 589 nm, 4s constant light) and the previously paired auditory cue but no pellet delivery. Each completed trial on the stim- lever (previously pellet alone) resulted in the delivery of its auditory cue but no pellet itself. At the end of the session total number of lever presses on the stim+ and stim-, as well as the number of rewards received were collected and plotted.

Laser extinction phase. After receiving reminder acquisition training with stim+ versus stim- for 2 days, rats underwent 4 consecutive days of laser-extinction, to test the persistence of laser-induced preference.

During laser extinction sessions, each completed trial (RR4) on the stim+ lever resulted in delivery of a food pellet and the previously paired auditory cue but no laser stimulation. Each completed trial on the stim- lever resulted in delivery of the pellet and its auditory cue. Thus, during these sessions, the outcome for both levers consisted in the delivery of a pellet and the associated auditory cue, with no administration of laser stimulation. At the end of the session total number of lever presses on the stim+ and stim-, as well as the number of rewards received were collected and plotted.

Normal chow consumption

We next examined the effect of laser stimulation on voluntary normal chow consumption in a 30-minute chow consumption test. Intake test was conducted in a familiar chamber (similar to the home cage) containing bedding on the floor in which rats had serial access to pre-weighed quantities of regular chow pellets (20 g) while also having constant access to water. Intake tests were repeated on 3 consecutive days. Laser stimulation was administered only on 1 day (optical activation: 473nm, 20Hz, light pulses of 25ms, 50% duty cycle, throughout the entire session; optical inhibition: 589 nm, constant light throughout the entire session; both with 10mW at the tip of the implanted fiber), which occurred on either day 2 or 3 (counterbalanced across rats). Control intake was measured in the absence of any laser stimulation on the 2 remaining days (day 1 and either day 2 or 3, averaged together to form a baseline measurement). Chow was weighed at the end of the test to calculate the amount consumed.

Food pellets consumption

We examined the effect of laser stimulation on voluntary palatable food consumption in a 30-minute test food pellet consumption test. Intake test was conducted in a familiar chamber (similar to the home cage) containing bedding on the floor in which rats had serial access to pre-weighed quantities of food pellets (around 20 g) while also having constant access to water. Intake tests were repeated on 3 consecutive days. Laser stimulation was administered only on 1 day (optical activation: 473nm, 20Hz, light pulses of 25ms, 50% duty cycle, throughout the entire session; optical inhibition: 589 nm, constant light, throughout the entire session; both with 10mW at the tip of the implanted fiber), which occurred on either day 2 or 3 (counterbalanced across rats). Control intake was measured in the absence of any laser stimulation on the 2 remaining days (day 1 and either day 2 or 3, averaged together to form a baseline measurement). Food pellets were weighed at the end of the test to calculate the amount consumed.

Food preference

We examined the effect of laser stimulation on voluntary food preference in a 90 min free-intake test. Intake tests were conducted in a familiar chamber (similar to the home cage) containing bedding on the floor in which rats had serial access to pre-weighed quantities of chow (20 g) and food pellets (about 20 g), while also having constant access to water. Each food intake session consisted of 30 min access to 20 g of chow followed by 60 min of access to about 20 g of food pellets and chow. Intake tests were repeated on 3 consecutive days. Laser stimulation was administered only on 1 day (optical activation: 473nm, 20Hz, light pulses of 25ms, 50% duty cycle, throughout the entire session; optical inhibition: 589 nm, constant light throughout the entire session; both with 10mW at the tip of the implanted fiber), which occurred on either day 2 or 3 (counterbalanced across rats). Control intake was measured in the absence of any laser stimulation on the 2 remaining days (day 1 and either day 2 or 3, averaged together to form a baseline measurement). Chow and food pellets were weighed at the end of the test to calculate the amount consumed.

Optogenetic manipulation

Optical manipulation for PR and two-choice schedule of reinforcement tasks was performed using either a 473 nm (ChR2) or 589 nm (NpHR) DPSS lasers, which were controlled by the MedPC software (Med Associates), through a pulse generator (Master-8; AMPI, New Ulm, MN, USA).

Before all behavioral sessions, rats were connected to an opaque optical fiber, through previously implanted ferrules placed unilaterally in the VP.

Optical stimulation was performed as follows: 473nm, 1s at 20Hz, 20 light pulses of 25ms, 50% duty cycle; 10 mW at the tip of the implanted fiber.

Optical inhibition was performed as follows: 589 nm; 4s continuous light of 10 mW at the tip of the implanted fiber.

In vivo single cell electrophysiological recordings

Three weeks post-surgery, D2-ChR2 rats and D2-NpHR ($n = 4/\text{group}$) were anaesthetized with urethane (1.44 g kg^{-1} , Sigma). The total dose was administered in three separate intraperitoneal injections, 15 min apart. Adequate anesthesia was confirmed by the lack of withdrawal responses to hindlimb pinching. A recording electrode coupled with a fiber optic patch cable (Thorlabs) was placed in the VP (coordinates from bregma: 0 to -0.10 mm AP , $+2.3$ to $+2.5 \text{ mm ML}$, and -7 to -7.6 mm DV).

Single neuron activity was recorded extracellularly with a tungsten electrode (tip impedance 5–10 M Ω at 1 kHz) and data sampling was performed using a CED Micro1401 interface and Spike2 software (Cambridge Electronic Design).

The DPSS 473 nm or 589 nm laser systems, controlled by a stimulator (Master-8, AMPI) was used for intracranial light delivery. Optical stimulation was performed as follows: 473nm, 1s at 20Hz, 20 light pulses of 25ms, 50% duty cycle, 10 mW at the tip of the fiber. Optical inhibition was performed as follows: 589 nm, 4sec of constant light, 10 mW at the tip of the fiber.

Firing rate histograms were calculated for the baseline (10 s before stimulation), stimulation period and after stimulation period (10 s after the end of stimulation).

In order to calculate the PSTH, each recorded spike train (each train of 1sec) from a single neuron was aligned by the onset of optical stimulation. For plotting the normalized firing rate, r_i , the average activity during baseline was subtracted to each spike train ($r_i = r_i - \text{avg}(r_i | t < 10\text{s})$). The neurons were considered as responsive or not responsive to the stimulation on the basis of their firing rate change with respect to the baseline period. Neurons showing a firing rate increase or decrease by more than 20% from the mean frequency of the baseline period were considered as responsive (Benazzouz et al., 2000; Soares-Cunha et al., 2016b).

VP neurons were identified as those having a baseline firing rate between 0.2 and 18.7 Hz (Richard et al., 2016). Other non-identified neurons (corresponding to less than 10% of recorded cells) were excluded from the analysis.

Immunofluorescence

Rats were deeply anesthetized with pentobarbital (Eutasil) and were transcardially perfused with 0.9% saline followed by 4% paraformaldehyde. Brains were removed and post-fixed in 4% paraformaldehyde for 24 hours. Afterwards, brains were transferred to a 30% sucrose solution (for at least 48h), and then prepared for sectioning. Coronal sections (50 μm) of NAc and VP were obtained by vibratome sectioning.

Coronal 50 μm vibratome sections (at least 5 sections per animal) were pretreated for antigen retrieval with citrate buffer (0.1M, pH 6.0), rinsed in phosphate-buffered saline (PBS), permeabilized with 0.3% triton x-100 in PBS for 10 min, blocked with 5% fetal bovine serum for 2 h at room temperature and incubated for 48 h at room temperature with polyclonal mouse anti-D2R (1:400, Santa Cruz

Biotechnology, catalog #sc-5303, RRID: [AB_668816](#)), Afterwards, sections were washed and incubated with the secondary antibody alexa fluor 594 donkey anti-mouse (1:500, Thermo Fisher Scientific; catalog #A-21203, RRID: [AB_141633](#)) for 2 h. Afterwards, sections were washed and incubated with polyclonal goat anti-GFP (1:500, Abcam; catalog #ab6673, RRID: [AB_305643](#)) overnight at 4°C. Following, sections were washed, incubated with the secondary antibody alexa fluor 488 donkey anti-goat (1:500, Thermo Fisher Scientific; catalog #A-11055, RRID: [AB_142672](#)) for 2 h, and washed again. Finally, all sections were stained with 4',6-diamidino-2-phenylindole (DAPI, 1 mg ml⁻¹, Thermo Fisher Scientific, catalog #1306, RRID: [AB_2629482](#)) and mounted using an aqueous mounting medium (Permafluor, catalog #TA-030-FM, Thermo Fisher Scientific).

Images were collected and analyzed by confocal microscopy (Olympus LPS Confocal FV3000, Olympus). Estimation of cell density was done using one field of view of NAc, per coronal section, obtained with 20X magnification (636.4x636.4µm images). Cell counts were normalized to the area of the images.

QUANTIFICATION AND STATISTICAL ANALYSIS

Prior to any statistical comparison between groups, normality tests (Kolmogorov-Smirnov) were performed for all data analyzed, and appropriate statistical analysis was applied accordingly. Comparison between two groups was made using Student's t-test; when normality assumptions were not met Mann-Whitney was performed instead. Comparison between ON and OFF behavioral sessions of the same group were performed using paired t-test; when normality assumptions were not met Wilcoxon was performed instead). Mixed-effects analysis of variance (ANOVA) was used to compare groups (D2-ChR2, D2-NpHR, D2-YFP) and sessions (OFF vs ON; stim+ vs stim-; cue vs reward); One way ANOVA for repeated measures was used to compare firing rate before, during and after stimulation; Bonferroni's *post hoc* multiple comparisons was used for group differences determination (when normality assumptions were not met Friedman's test was performed, and Dunn's multiple comparison for *post hoc* analysis).

For the analysis of normalized electrophysiological temporal activity (through PSTH), Kolmogorov-Smirnov for 2 samples was performed to determine differences between the distribution of the stimulus period and the average baseline activity.

Results are presented as mean ± SEM. All of the statistical details of experiments can be found throughout the results description; these include the statistical tests used and p-value. The n for each experiment is indicated in the figures' legends.

All statistical analysis was performed using GraphPad (Prism 7, La Jolla, CA, USA).

Cell Reports, Volume 38

Supplemental information

**Distinct role of nucleus accumbens D2-MSN
projections to ventral pallidum in different
phases of motivated behavior**

Carina Soares-Cunha, Ana Verónica Domingues, Raquel Correia, Bárbara Coimbra, Natacha Vieitas-Gaspar, Nivaldo A.P. de Vasconcelos, Luísa Pinto, Nuno Sousa, and Ana João Rodrigues

Supplemental Information

Table S1. Statistical table of main figures, Related to Figures 1, 2, 3 and 4.

Figure	Test	Test value	p value
Figure 1E	One-way ANOVA	$F_{(2,29)} = 7.32$	$p = 0.0083$
Figure 1F (type A)	Kolmogorov-Smirnov	$D = 1.0$	$p = 0.0286$
Figure 1F (type B)	Kolmogorov-Smirnov	$D = 1.0$	$p < 0.0001$
Figure 1H	Two-way ANOVA	Group: $F_{(1,17)} = 0.1283$ Day of training: $F_{(5,85)} = 114.3$	$p = 0.7246$ $p < 0.0001$
Figure 1I	Mixed Two-way ANOVA	Group: $F_{(3,34)} = 93.10$ Day of training vs cue/reward: $F_{(21,238)} = 8.82$	$p < 0.0001$ $p < 0.0001$
Figure 1J	Mixed Two-way ANOVA	Group: $F_{(1,34)} = 10.29$ Group vs ON/OFF: $F_{(1,34)} = 6.267$	$p = 0.0028$ $p = 0.0173$
Figure 1K	Unpaired t test	$t_{17} = 3.798$	$p = 0.0014$
Figure 1L	Mixed Two-way ANOVA	Group: $F_{(1,9)} = 8.46$ ON vs OFF: $F_{(1,7)} = 6.258$	$p = 0.0173$ $p = 0.0409$
Figure 2D (type A)	Kolmogorov-Smirnov	$D = 0.7273$	$p = 0.0059$
Figure 2D (type B)	Kolmogorov-Smirnov	$D = 0.7059$	$p = 0.0004$
Figure 2F	Two-way ANOVA	$F_{(1,17)} = 0.1718$	$p = 0.6837$
Figure 2G	Mixed Two-way ANOVA	Group: $F_{(3,34)} = 0.1283$ Day of training: $F_{(21,238)} = 8.5$	$p < 0.0001$ $p < 0.0001$
Figure 2H	Mixed Two-way ANOVA	Group: $F_{(1,9)} = 4.89$ Group vs cue/reward: $F_{(1,6)} = 10.37$	$p = 0.0543$ $p = 0.0181$
Figure 2I	Unpaired t test	$t_{16} = 4.04$	$p = 0.0009$
Figure 2J	Two-way ANOVA	Group: $F_{(1,9)} = 4.56$ ON vs OFF: $F_{(1,5)} = 8.348$	$p = 0.0614$ $p = 0.0342$
Figure 3B	Mixed Two-way ANOVA	Group: $F_{(1,9)} = 5.2$ Group vs cue/reward: $F_{(1,5)} = 20.8$	$p = 0.0485$ $p = 0.0061$
Figure 3C	Mann Whitney test	$U = 3.5$	$p = 0.0003$
Figure 3C'	Mixed Two-way ANOVA	Group: $F_{(1,9)} = 2.123$ cue vs reward: $F_{(1,9)} = 2.123$	$p = 0.1791$ $p = 0.0002$
Figure 3D	Mixed Two-way ANOVA	Group: $F_{(1,34)} = 2.082$ ON vs OFF: $F_{(1,34)} = 8.84$	$p = 0.1582$ $p = 0.0054$
Figure 3F	Mixed Two-way ANOVA	Group: $F_{(1,9)} = 38.71$ Group vs cue/reward: $F_{(1,7)} = 29.3$	$p = 0.0002$ $p = 0.0010$
Figure 3G	Mann Whitney test	$U = 0.0$	$p < 0.0001$
Figure 3G'	Mixed Two-way ANOVA	Group: $F_{(1,9)} = 12.47$ cue vs reward: $F_{(1,9)} = 56.2$	$p = 0.0064$ $p < 0.0001$
Figure 3H	Mixed Two-way ANOVA	Group: $F_{(1,34)} = 27.71$ ON vs OFF: $F_{(1,34)} = 26.48$	$p < 0.0001$ $p < 0.0001$
Figure 4B	Two-way ANOVA	Group: $F_{(1,48)} = 54.4$ Group vs stim+/stim-: $F_{(7,48)} = 7.26$	$p < 0.0001$ $p < 0.0001$
Figure 4C	Two-way ANOVA	Group: $F_{(1,32)} = 29.3$ Group vs stim+/stim-: $F_{(7,32)} = 3.5$	$p < 0.0001$ $p = 0.0064$

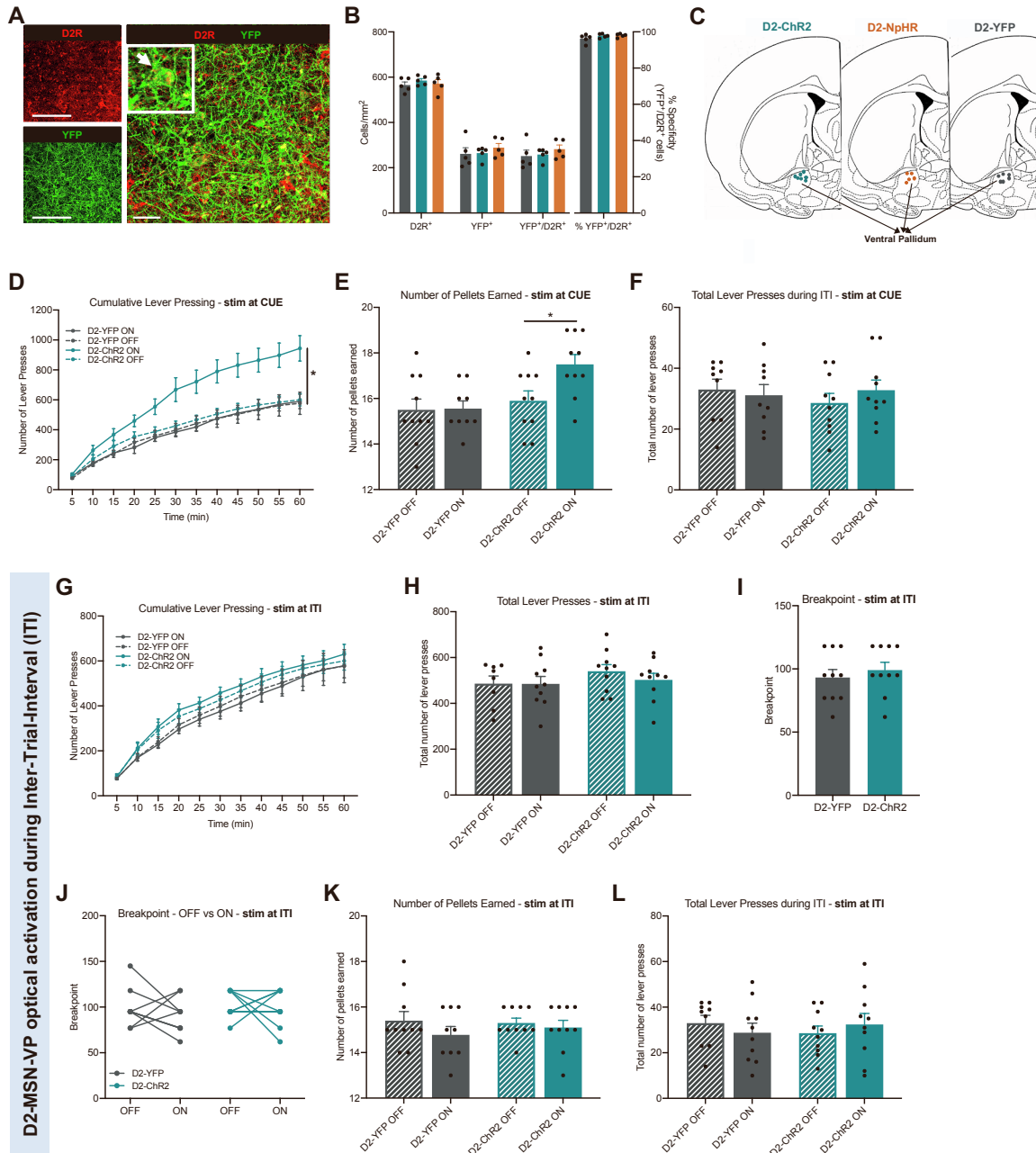


Figure S1. Optogenetic activation of D2-MSN-VP terminals during cue exposure increases motivation, Related to Figure 1.

A Representative immunostaining for D2R and YFP in the NAC of an animal injected with AAV5-D2R-ChR2(H134R)-eYFP; scale bar: 50 μ m; inset showing a double-stained neuron (identified with white arrow).

B Quantification of the number of D2R⁺ and YFP⁺ cells per area as evaluated by IF; almost all of YFP⁺ cells are also D2R⁺, confirming the specificity of the construct (n=5 animals/group).

C Schematic of optic fiber placement location of D2-ChR2, D2-NpHR and D2-YFP rats of experimental Group II. **D** Cumulative lever presses in the PR session with optical stimulation on cue, showing a significant higher number in the ON

session when comparing with the OFF session of D2-ChR2 rats (two-way ANOVA; Group differences: $F_{(3,34)}=7.78$, $p=0.0004$; Time X Group differences: $F_{(33,374)}=5.176$, $p<0.0001$; Bonferroni's *post hoc*, D2-ChR2 ON vs OFF, $p=0.0181$). **E** In the PR session with optical stimulation on cue D2-ChR2 rats earned significantly more food pellets (Group differences: $F_{(1,9)}=5.591$, $p=0.0423$). **F** Total number of lever presses performed during the inter-trial interval (ITI) of the PR session. **G-L** D2-MSN-VP terminal optical stimulation during inter-trial-interval (ITI), a period of time-out from the task, does not change **G** Cumulative lever presses, **H** total number of lever presses, **I-J** breakpoint, **K** the number of food pellets earned, or **L** the total number of lever presses performed during ITI in a PR session. $n_{D2-ChR2}=10$, $n_{D2-YFP}=9$. Error bars denote SEM. $*p \leq 0.05$.

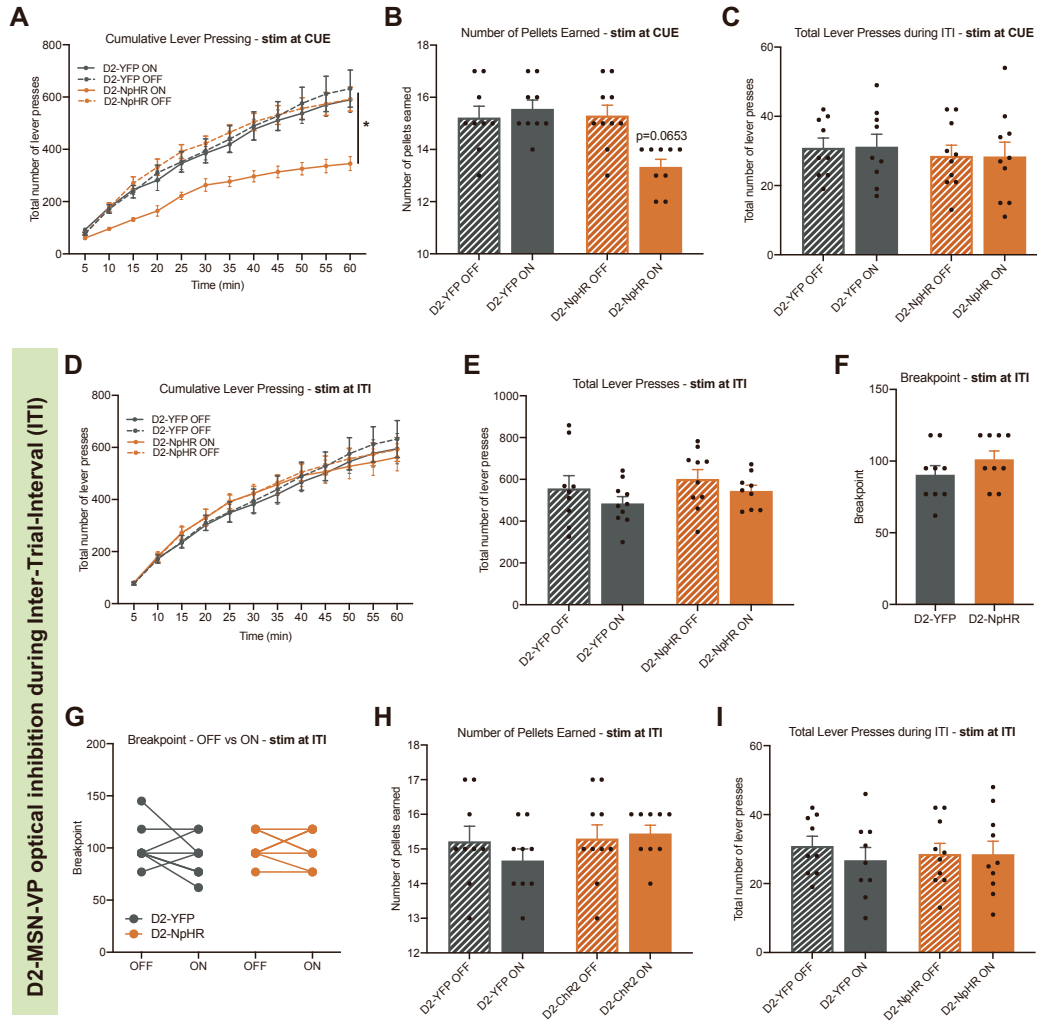


Figure S2. Optogenetic inhibition of D2-MSN-VP terminals during cue exposure decreases motivation, Related to Figure 2.

A Cumulative lever presses in the PR session with optical inhibition on cue, showing a significant difference between ON session and OFF session of D2-NpHR rats (two-way ANOVA; Group differences: $F_{(3,33)}=8.153$, $p=0.0003$; Time X Group differences: $F_{(33,363)}=3.369$, $p<0.0001$; Bonferroni's *post hoc*, D2-NpHR ON vs OFF; $p=0.0206$). **B** In the PR session D2-NpHR rats earned marginally less food pellets (Group differences: $F_{(1,9)}=11.12$, $p=0.0087$). **C** Total number of lever presses performed during the inter-trial interval (ITI) of the PR session. **D-I** D2-MSN-VP terminal optical inhibition during inter-trial-interval (ITI), a period of time-out from the task, does not change **D** the cumulative lever presses, **E** the total number of lever presses, **F-G** breakpoint, **H** the number of food pellets earned, or **I** the total number of lever presses performed during ITI in a PR session. $n_{D2-NpHR}=10$, $n_{D2-YFP}=9$. Error bars denote SEM.

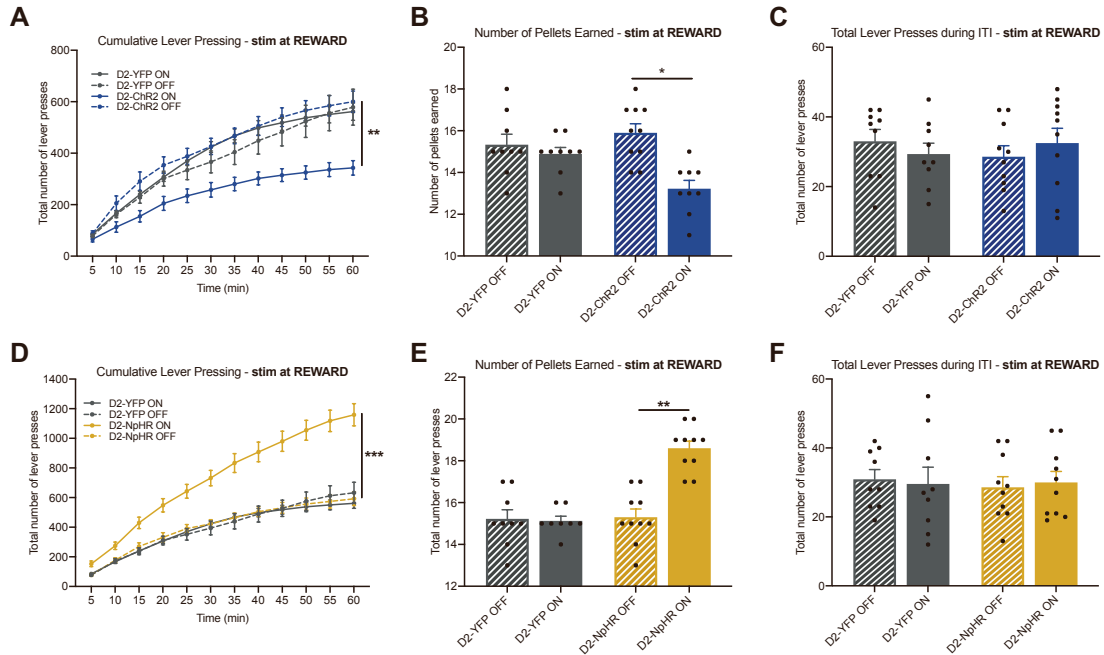


Figure S3. Optogenetic modulation of D2-MSN-VP terminals at reward delivery alters motivation, Related to Figure 3.

A Cumulative lever presses in the PR session with optical activation at reward delivery (two-way ANOVA; Group differences: $F_{(3,34)}=7.54$, $p=0.0005$; Time X Group differences: $F_{(33,374)}=4.505$, $p<0.0001$; D2-ChR2 ON vs D2-ChR2 OFF, Bonferroni's *post hoc*, $p<0.0001$). **B** Number of food pellets earned during the PR session with optical stimulation at reward delivery (Group differences: $F_{(1,9)}=3.623$, $p=0.0891$). **C** Total number of lever presses performed during ITI the PR session with optical stimulation at reward delivery. **D** Cumulative lever presses in the PR session with optical inhibition at reward delivery (two-way ANOVA; Group differences: $F_{(3,34)}=21.55$, $p<0.0001$; Time X Group differences: $F_{(33,374)}=14.80$, $p<0.0001$; D2-NpHR ON vs D2-NpHR OFF, Bonferroni's *post hoc*, $p<0.0001$). **E** Number of food pellets earned during the PR session with optical inhibition at reward delivery (Group differences: $F_{(1,9)}=1.453$, $p=0.2587$). **F** Total number of lever presses performed during ITI the PR session with optical inhibition at reward delivery. $n_{D2-ChR2}=10$; $n_{D2-NpHR}=10$, $n_{D2-YFP}=9$. Error bars denote SEM. * $p \leq 0.05$; ** $p \leq 0.01$; *** $p \leq 0.001$.

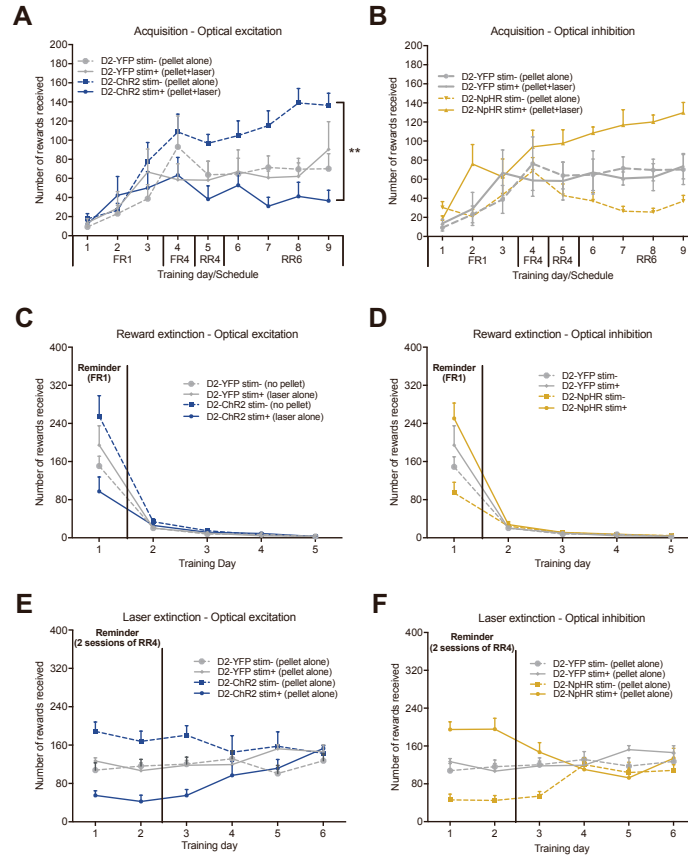


Figure S4. Optical activation/inhibition of D2-MSN-VP terminals paired with reward delivery reduces/increases preference and decreases/increases motivation, Related to Figure 4.

Number of rewards received in the acquisition phase with **A** optical excitation (two-way ANOVA, $F_{(7, 48)}=37.15$, $p<0.001$; Bonferroni's post hoc, D2-ChR2 stim+ vs D2-ChR2 stim-, $p<0.001$) and **B** optical inhibition (two-way ANOVA, $F_{(8, 54)}=6.286$, $p<0.001$; Bonferroni's post hoc, D2-NpHR stim+ vs D2-NpHR stim-, $p<0.001$). Number of rewards received in the reward extinction phase with **C** optical excitation and **D** optical inhibition. Number of rewards received in the laser extinction phase with **E** optical excitation and **F** optical inhibition. $n_{D2-ChR2}=7$; $n_{D2-NpHR}=5$, $n_{D2-YFP}=6$. Error bars denote SEM. * $p \leq 0.05$; ** $p \leq 0.01$.

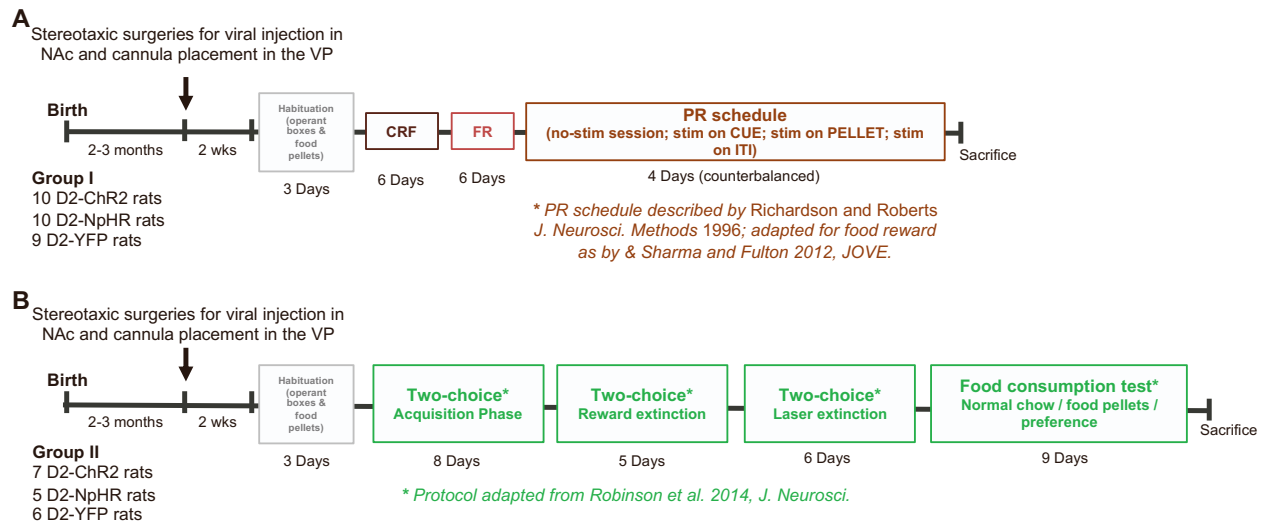


Figure S5. Experimental design, Related to Figures 1, 2, 3 and 4.

A Animals from Group I were subjected to stereotaxic surgeries for injection of D2-ChR2, D2-eNpHR or D2-YFP in the nucleus accumbens (NAc) and optic fiber placement in the ventral pallidum (VP). After recovering, animals performed the progressive ratio task (PR); on the PR test sessions, rats received one session without optical manipulation, one session with optical manipulation at cue, one session with optical manipulation at reward delivery and one session with optical manipulation at inter-trial interval (ITI). **B** Animals from Group II were subjected to stereotaxic surgeries for injection of D2-ChR2, D2-NpHR or D2-YFP in the NAc and optic fiber placement in the VP. After recovering, animals performed the two-choice schedule of reinforcement, followed by the normal chow food consumption test, the food pellet consumption test and the food preference (normal chow vs food pellet) test.

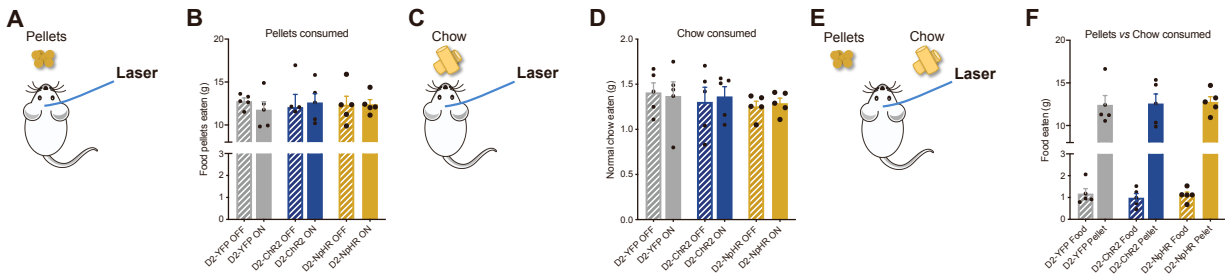


Figure S6. Optogenetic modulation of D2-MSN-to-VP terminals does not change food consumption, Related to Figure 4. **A** Optogenetic modulation was performed during a free consumption behavioral session for food pellets. **B** The amount of food pellets consumed was similar between a session with optical modulation (ON session) and a session with no optical modulation (OFF session) for all groups. **C** Optogenetic activation or inhibition was given during a free consumption behavioral session for regular chow. **D** the amount of chow consumed was similar between a session with optical modulation (ON session) and a session with no optical modulation (OFF session) for all groups. **E** Optogenetic activation or inhibition was given during a free consumption behavioral session in which rats could chose to consume both food pellets and regular chow. **F** All rats preferred to consume food pellets, irrespective of the experimental group. $n_{ChR2}=5$, $n_{D2-NpHR}=5$, $n_{D2-YFP}=5$. Error bars denote SEM.